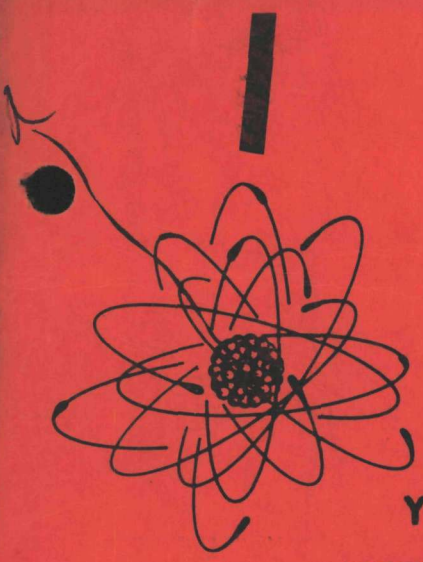

YAEC-136

YANKEE ATOMIC ELECTRIC COMPANY
RESEARCH AND DEVELOPMENT PROGRAM

THE NUCLEAR DESIGN OF THE YANKEE CORE

R & D SUBCONTRACT NO.1 UNDER
USAEC-YAEC CONTRACT AT(30-3)-222

FEBRUARY 1961

WESTINGHOUSE ELECTRIC CORPORATION
ATOMIC POWER DEPARTMENT
PITTSBURGH,30 P. O. BOX 355 PENNSYLVANIA

YAEC-136

Yankee Atomic Electric Company

Research And Development Program

THE NUCLEAR DESIGN OF THE YANKEE CORE

By

H. W. Graves, Jr.
R. F. Janz
C. G. Poncelet

Nuclear Engineering Section
Reactor Development

**For The Yankee Atomic Electric Company
Under Research and Development Subcontract
No. 1 of USAEC-YAEC Contract AT(30-3)-222**

February 1961

APPROVED: 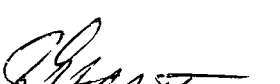

W. E. Abbott, Manager
Reactor Development

Westinghouse
ELECTRIC CORPORATION
ATOMIC POWER DEPARTMENT
P.O. BOX 355
PITTSBURGH 30, PA.

DISCLAIMER

TABLE OF CONTENTS

TABLE OF CONTENTS (Continued)

LIST OF FIGURES

LIST OF TABLES

ABSTRACT

This report describes the nuclear characteristics of the initial core loading for the Yankee Atomic Electric Company power plant. These include core reactivity, control rod and boron worths, and reactivity coefficients. In addition to operating characteristics, parameters for the cold and hot zero power cores are obtained for comparison with startup experiment data. Calculations to determine these characteristics are based on final mechanical design specifications.

1.0 INTRODUCTION

When the Research and Development Program for the Yankee Atomic Electric Plant was initiated in 1956, the preliminary reactor design made use of several unique features which, up to that time, had not been incorporated in previous reactors, and on which very little basic information was available. Yankee was the first reactor to make use of pressurized light water, stainless steel, and slightly enriched UO_2, a combination of material which yields a very hard thermal neutron spectrum, and a significant fraction of epithermal fissions in U-235. It was also the first reactor to make use of a soluble neutron poison in the moderator to provide shutdown at ambient temperatures. Control rod worth suffers considerably in a hard spectrum thermal reactor because of the low thermal neutron diffusion length. The use of a chemical shutdown system in the Yankee reactor reduced the control rod requirements by roughly a factor of two.

Since little reactor physics information was available for low enrichment reactors with such a hard neutron spectrum, one of the objectives of the Research and Development program was to obtain, by both analysis and experiment, a thorough understanding of the reactor physics aspects of stainless steel - UO_2-light water reactor cores. The program consisted of both experimental and analytical studies. A series of part-core critical experiments were carried out at the Westinghouse Reactor Evaluation Center in Waltz Mill, Pa. [1,2]. These experiments provided data which were used as "bench marks" to verify the analytical methods being developed and evaluated at the Westinghouse Atomic Power Department in Forest Hills, Pa. The results of the experiments, and several comparisons of reactor theory with experiment[3,4,5] have been described in previous reports.

An additional objective of the program was to arrive at an optimum analytical design for the Yankee core. The physics design of the first core was based on the following ground rules:

1. A core size and a maximum-to-average fission power density such that the reactor would have a capability of 392 Mw thermal throughout life without exceeding thermal limitations of the fuel [6].

2. A core life of 10,000 hours at 392 Mw thermal.

3. Sufficient reactivity control in the form of control rods to provide 3% Δk_{eff} shutdown in the hot, clean, zero power core.

4. Sufficient reactivity control in the form of both control rods and boric acid dissolved in the moderator to provide 5% Δk_{eff} shutdown in the cold, clean, zero power core.

It was found that 24 cruciform control rods with a span of 7.865 inches and a thickness of .265 inches would satisfy the hot control requirement and still permit sufficient excess reactivity to yield the desired core lifetime. To account for reactivity uncertainties, provision has also been made to insert eight fixed cruciform neutron poison shim elements which can be used to reduce the excess reactivity of the core. Studies of reactivity, lifetime and power distributions have been carried out and the results presented in previous reports [7,8,9]. It is the object of this report to present the most up-to-date values for the reactivity and control characteristics, as well as the kinetic characteristics of the Yankee reactor. These values have all been calculated using final assembly drawings for all dimensions and material compositions obtained during fabrication of fuel assemblies. A description of the mechanical design is presented in Section 2.

The reactivity characteristics of the core were evaluated using the MUFT-SOFOCATE-WANDA system of computer codes developed at the Bettis Atomic Power Laboratory. A semi-empirical method has been developed to provide input to the codes which takes account of the heterogeneity of the Yankee fuel lattice. This method has been quite successful in predicting results of the Yankee part-core critical experiments, as well as a large numberof other critical experiments performed on light water moderated, low enrichment lattices. Section 3 contains a description of the method, and its application to the Yankee core.

The core characteristics presented in Sections 4 and 5 allow the evaluation of clean core reactivity, control rod worth, and boron worth and a determination of their interaction. Some of the information presented was evaluated to provide a comparison with the experimental data generated during startup experiments.

In addition to a determination of basic reactivity and total control characteristics, control rod group worths for the reference control rod program have been evaluated to determine rod movements required for various operating conditions. Reactivity changes associated with xenon, samarium, and U-238 Doppler effects have also been evaluated for various power levels and control rod configurations. The latter variable must be considered because of the dependence of power distribution and neutron importance on control rod distribution.

Section 6 contains a discussion of the kinetic characteristics of the core. These include the moderator temperature coefficient, Doppler and power coefficients, pressure and void coefficients, and prompt neutron lifetime. In all cases, the coefficients have been calculated for a critical core, and the effects of both control rods and chemical poison on the coefficients are evaluated.

Section 7 contains a tabular summary of the nuclear characteristics of the Yankee first core.

2.0 DESCRIPTION OF CORE

2.1 Mechanical Design

The initial core for the Yankee Reactor can be approximated by a right circular cylinder 75.4 inches in diameter and 91.85 inches high (68°F), with a length-to-diameter ratio of 1.2. The core consists of 76 vertical fuel assemblies, 24 control rods, and 8 fixed shim elements. The fuel assemblies are essentially square in cross section and are placed in a close-packed square lattice. Figure 2.1 shows a cross section of the core.

The basic fuel element for the first core is composed of 0.340 inch O.D. stainless steel tubes, which contain uranium dioxide fuel in the form of cylindrical ceramic pellets. The pellets are 0.294 in. in diameter and 0.6 in. long. The pellets are produced by sintering a powder-compact of slightly enriched UO_2. The required diametrical dimensional tolerances for the individual pellets are obtained by centerless grinding after sintering. The uranium is enriched in the fissionable isotope U-235 to 3.40 w/o.

The fuel tubes are Type 348 stainless steel with a wall thickness of 0.021 in. The pellets are placed in the fuel tubes in groups of 25 with a total of six groups. Each group is separated from the next by a perforated stainless steel disc. Each disc has a circumferential groove into which the tube is crimped during the pellet loading process (fixing its position). The discs are so spaced that each group of 25 pellets is allowed a free expansion space. Thus, the active fuel height contains the pellet stack of 90 inches, plus the 6 spacer discs of .121 in. thickness and the 6 expansion spaces of .187 in. thickness, bringing the active length of the core to 91.85 inches.

The fuel rods are assembled on a square lattice with a normal center-to-center pitch of 0.422 in. and on an odd pitch of 0.454 in. for those rows of tubes in line with the control rod vanes. Two final assembly designs are used which contain 304 and 305 fuel rods, respectively. Each assembly is basically a 18 by 18 rod square. Rods are omitted from this

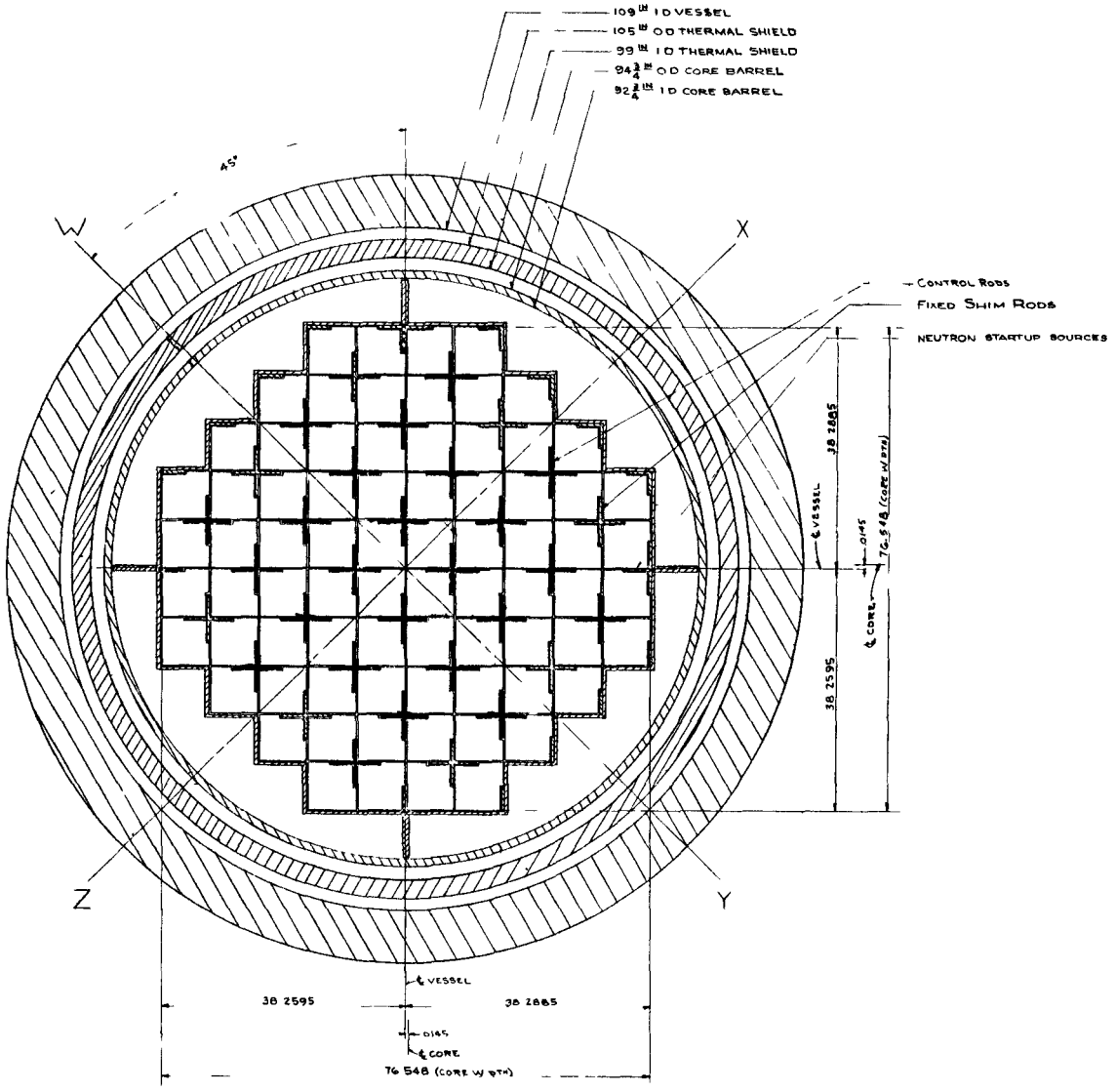

CORE CROSS SECTION

Figure 2.1

pattern as required to provide slots for passage of the vanes of the cruciform control rods, and to permit the insertion of an instrumentation channel in the center of the assembly (.375 inch O.D., .065 inch wall thickness), thereby reducing the number of rods from 324, the number in the full 18 by 18 complement, to 304 and 305. The total number of rods which form the 76 fuel assemblies is 23,142. The fuel rods and instrumentation channels are properly oriented by the use of tubular spacers, termed "ferrules," of 1/2 inch length, which are brazed to the fuel rods at 8 inch axial intervals.

A fuel assembly is built up from 9 sub-assemblies tied together by tie straps. Rubbing straps are brazed to the outer tube row of an assembly at four axial positions to prevent undesirable rubbing of a control rod on a row of fuel tubes and to eliminate fuel rod surface contact between assemblies. The detailed design of the fuel assemblies is shown in Figure 2.2. Each fuel assembly has a total length of 111.25 inches, with a total fuel length of 91.85 inches. The assemblies approximate a 7.61 inch square in cross section.

The 24 control rods are cruciform in shape. The control rods are fabricated from a silver-indium-cadmium alloy (80% Ag., 15% In., 5% Cd.). The rods are plated with 0.001 inches of nickel for protection against corrosion. The neutron scattering introduced by this coating is negligible in its effect on rod worth. Connected to the active portion of the control rod is a Zircaloy-2 follower which acts as a guide and prevents the formation of a "water slot" in the core when the control rod is withdrawn.

In the reactor core, the types of fuel assemblies are limited to two, in order to simplify the fabrication process and the loading of the core. This results in a core having 32 cruciform slots plus a number of slots along the periphery of the core at the inside surface of the baffle. The latter slots contain stainless steel "vanes" and "fillers" (Figure 2.1). Twenty-four of the cruciform slots are occupied by movable control rods. The remaining 8 cruciform slots are filled with fixed shim elements consisting of a boron stainless steel section (Type 304L stainless steel - 1.35 w/o natural boron) and a Zircaloy-2 section with the same dimensions as the movable control rods. Each end of the rod is mechanically identical with

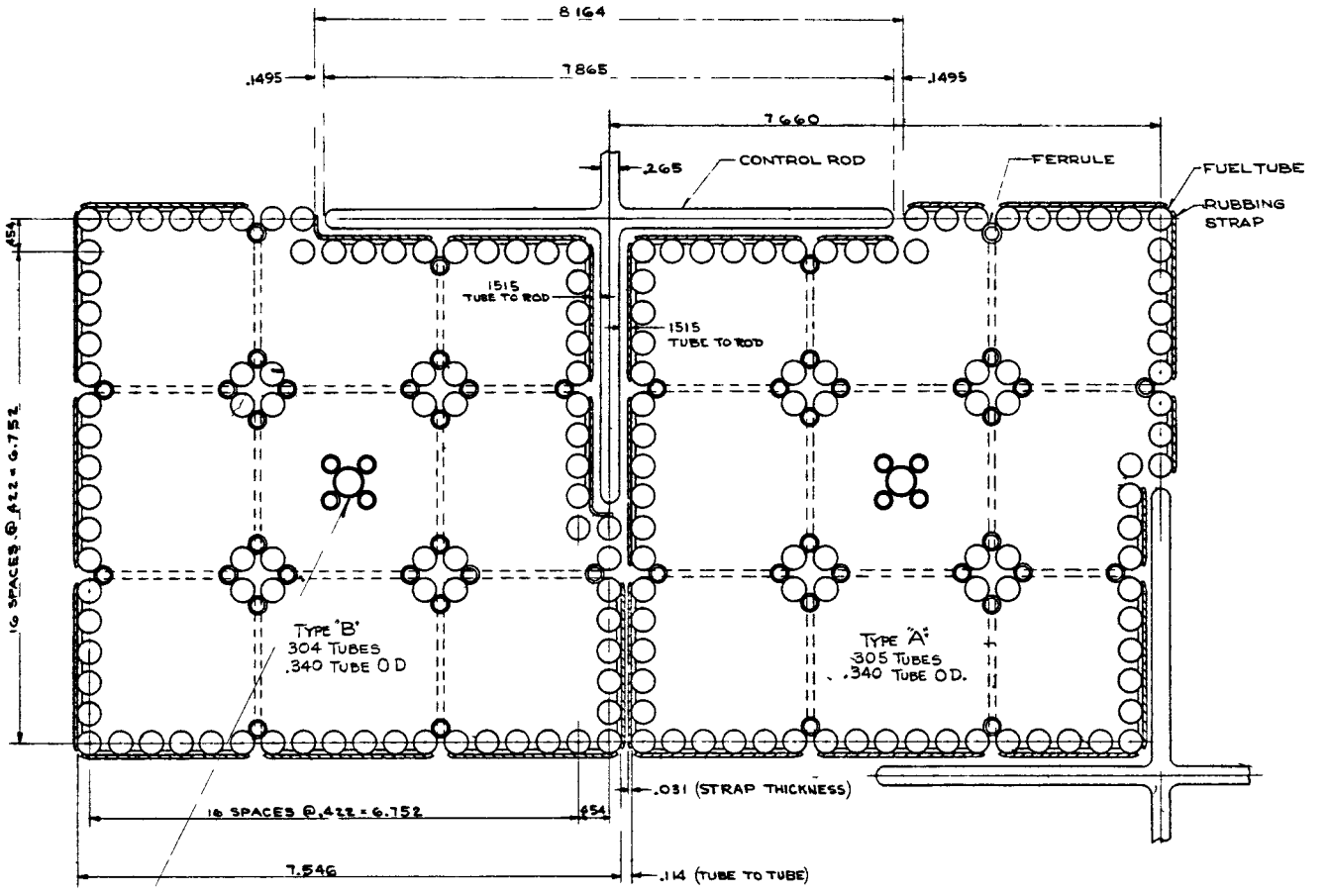

FUEL ELEMENT CROSS SECTION

1. 76 FUEL ASSEMBLIES
   38 TYPE A FUEL ASSEMBLIES
   38 TYPE B FUEL ASSEMBLIES
2. 32 CRUCIFORM SLOTS
   24 CONTROL RODS
   8 FIXED SHIM RODS
3. TOTAL FUEL TUBES (FULL CORE) = 23,142

Figure 2.2

the other, so that the rod may be inverted and either section may be used in the core. If little or no absorption effect is desired from fixed elements, Zircaloy-2 will be placed in the core with the boron stainless steel section as the extension. If an absorption effect is required for reactivity shim, boron stainless steel may be placed in the core with Zircaloy-2 as the extension. In either case, the shim element will reduce the undesirable neutron flux peaking which would occur if the water were not excluded from the slots. The decision as to which material to use will be made on the basis of the initial critical tests. A summary of the core design data is given in Table 2.1. These dimensions yield a core with a volume of 416,100 in^3 and a volumetric composition which is 49.11% water, 34.50% UO_2, 12.07% stainless steel (10.89% cladding, .40% ferrules plus straps, .34% fillers, .24% disks, .11% instrumentation channels, .09% vanes), 2.91% Zircaloy-2 (or control rods) and 1.41% void.

2.2 Materials Specifications

Listed below are the compositions of the principal constituents present in the core*.

2.2.1 Structural Material

The material used to clad the fuel, the ferrules, spacer discs, rubbing straps, and instrumentation channels is Type 348 stainless steel. Several different heats of steel are present in the core with slightly different compositions. It was necessary, therefore, to use a weighted average composition based on the corresponding footages of each heat. The average chemical analysis of the steel used in the calculations is given in Table 2.2.

---

* Material specifications and final dimensions were obtained from the fabrication group shortly after completion of core fabrication.

Table 2.1

YANKEE REACTOR DESIGN DATA

Core Description	
Average Core Diameter (cold)	75.4 in.
Active Core Length (cold)	91.85 in.
Number of Fuel Assemblies	76
UO_2 in the Core	52,334 lbs.
Uranium Enrichment	3.40 w/o
Fuel Design Data (cold dimensions)*	
Pellet Diameter	0.294 in.
Pellet Length	0.6 in.
Avg. UO_2 Density	10.18 gms/cm^3
Fuel Tube Material	Type 348 S.S.
Fuel Tube O.D.	0.340 in.
Fuel Tube I.D.	0.298 in.
Fuel Tube Center-to-Center Pitch - Normal	0.422 in.
- In line with control vanes	0.454 in.
Total Number of Fuel Rods	23,142
Control Rod Data	
Number of Movable Control Rods	24
Control Rod Material	80% Ag, 15% In, 5% Cd.
Control Rod Shape	Cruciform
Control Rod Span (cold)	7.865 in.
Control Rod Thickness (cold)	0.265 in.
Number of Shim Elements** (Zr-2 or Boron Steel)	8
Thermal and Hydraulic Design Data	
Coolant Flow, Total Rate, lb/hr	37.8 x 10^6
Operating Pressure, Normal, psi gage	2000
Pressure Drop Across Core, psi gage	16
Average Heat Transfer Flux, Btu/hr-ft^2	86,300
"Active" Heat Transfer Surface, ft^2	15,500
Temperature, °F	
Coolant in the Main Coolant System, Average	514
Coolant Rise in Core, Average	33
Film Drop, Average	14.3

* Tolerances on fuel design data may be found in reference 14.

** Same dimensions as movable control rods.

Table 2.2

WEIGHTED AVERAGE COMPOSITION OF STAINLESS STEEL

Element	w/o
Fe	67.13
Cr	18.28
Ni	10.95
Mn	1.74
Nb	.90
Si	.78
C	.07
Co	.063
Ta	.056
P	.020
S	.015

2.2.2 Fuel

The fuel consists of slightly enriched uranium compounded in the form of UO_2. The fuel in the reactor was obtained from two sources, with the chemical analyses given in Table 2.3.

Table 2.3

CHEMICAL COMPOSITION OF UO_2 PELLETS

Analysis	Mallinckrodt	(W) AFD	Weighted Avg.
U-235/U (w/o)	3.391%	3.406%	3.399%
Total U (w/o)	88.07%	88.05%	88.06%
O/U (atomic ratio)	1.996	1.98	1.988

The weighted average is based on an equal mixture of the respective loadings of the two vendors' pellets.

An average chemical analysis of the impurities present in the two sources of fuel is given in Table 2.4, together with the corresponding thermal macroscopic absorption cross sections,

homogenized over the core. The total cross section represents a decrease in core reactivity of 0.06%. The reactivity calculations described in subsequent sections of this report neglected the effect of impurities.

Table 2.4

IMPURITY ANALYSIS OF UO_2 PELLETS

Impurity	$(ppm)_{average}$	Σ_a $(10^5$ $cm^{-1})$*
Al	77.3	.140
B	.21	3.102
Bi	.61	---
Cd	.51	3.18
Co	1.1	.146
Cr	50.5	.596
Cu	19.9	.250
Fe	567.	5.437
In	1.	.350
Mn	3.1	.158
N	800.**	22.73
Ni	63.4	10.52
Pb	1.	---
Si	131.7	.129
Ti	5.	.124
W	20.	.442
Zn	20.	.069
	Total	47.4

* Evaluated at 2200 m/sec.

** The concentration of N may be high - the experimental analysis was not conclusive.

2.2.3 Control Rod Followers

The control rod followers consist of an alloy of zirconium-Zircaloy-2. The weighted average composition of several heats of the Zircaloy in the core is given in Table 2.5.

Table 2.5

WEIGHTED AVERAGE COMPOSITION OF ZIRCALOY-2

Element	w/o
Zr	98.27
Sn	1.43
Fe	.10
Cr	.10
Ni	.04
Impurity	.06

In the calculations it was assumed that the control rod followers consisted of 100% zirconium. This assumption involves an underestimate of the thermal absorption cross section of the followers by about 10%. This difference, however, does not represent a significant effect on the reactivity of the core for two reasons:

(1) The followers make up less than 3% of the total core volume.

(2) The absorption cross sections of either the alloy or zirconium itself are small compared with other materials in the core.

3.0 METHODS OF ANALYSIS

The procedure used for criticality calculations is based on an extensive survey and analysis of critical lattice configurations carried out under the Yankee Research and Development program and described in Reference 4. This system of computational methods utilizes a sequence of hand calculations and computer programs for the computation of few-group macroscopic parameters which are used in diffusion theory calculations of multiplication factors.

3.1 Nuclear Constants

The heterogeneous array of fuel, stainless steel, water, control rod or control rod follower which makes up a characteristic fuel assembly in the reactor is divided, for purposes of computation, into three discrete regions: homogenized "fuel", control rod or control rod follower, and a water slot adjacent to the control rod or follower. The "fuel" consists of the UO_2 pellets, stainless steel cladding, ferrules, instrumentation channels, discs, and rubbing straps, and the water not included in the slot associated with the control rod or follower, all homogenized on a volume fraction basis.

The calculated material number densities in the homogenized "fuel" region are modified to account for spatial self shielding by the use of thermal flux disadvantage factors obtained from the I_2 computer program [10]. Flux weighted number densities in the "fuel" region are then used as input to the SOFOCATE code [11], developed at the Bettis Atomic Power Laboratory for the calculation of macroscopic thermal cross sections utilizing the method of Wigner and Wilkins [12]. The high energy limit chosen for the thermal neutron group is 0.625 ev. The SOFOCATE code provides, as output, the macroscopic thermal cross sections and diffusion coefficient needed for a diffusion theory calculation of criticality, as well as microscopic thermal cross sections averaged over the energy spectrum defined by the input number densities.

Group constants in the "fuel" region for non-thermal neutrons are calculated by means of the Bettis computer program MUFT IV [13]. This 54-group machine code is used to obtain spectrum averaged cross sections

for use in two group diffusion equations. The spectrum computed by the MUFT IV code is based on the assumption of one dimensional rectangular geometry with a group independent buckling.

The major uncertainty involved in the use of the MUFT IV code is associated with the specification of "self shielding factors" (L-factors) for use in calculating absorption in the resonances of both U-235 and U-238. An empirical scheme has been developed on the basis of a fit to a large number of critical experiments for the calculation of the ratio of resonance capture in U-238 to removal from the resonance group [4]. The MUFT IV code has been modified to carry out an "L-factor search" which permits the selection of an L-factor for U-238, adjusting the MUFT IV results to the empirical fit. The L-factor for U-235 was assumed to be unity (no resonance self-shielding). Few-group cross sections are then available as MUFT output data.

The thermal group cross sections in the control rod follower and water slot are obtained from the SOFOCATE calculations in the "fuel" region (Appendix A). The thermal energy spectrum in the water slot and follower are assumed to be the same as the spectrum in the "fuel".

Two sets of thermal constants are used in the control rod, depending on their application in a particular computer program (see Section 3.2). In one-dimensional diffusion theory calculations, where a control rod is represented by a discrete region, the thermal constants are based on a hand calculation for the diffusion length in the rod [28]. In analogous two-dimensional programs a ratio of thermal neutron current to flux at the surface of the rod, characteristic of a free boundary, is specified (.4695 cm^{-1}). No thermal neutron constants are required interior to the rod surface [17]

Fast group cross sections in the control rod follower and water slot are obtained by weighting three fast group microscopic cross sections with group averaged fluxes based on the fission spectrum in the Yankee core as calculated by the MUFT IV computer program. The three-group cross sections themselves have been obtained by comparing the macroscopic cross sections of homogeneous mixtures of the element of interest with a reference homogenized reactor core medium for several concentrations of this element.

A fast absorption cross section of 0.12 cm^{-1}, a diffusion coefficient of 1.0 cm. and a removal cross section of zero are used in the control rod. These values represent a fit to empirical data obtained in critical experiments [17].

The two-group constants for each of the discrete regions defined in the fuel assembly were obtained at the ambient and operating temperatures and several concentrations of chemical absorber.

3.2 Diffusion Theory Calculations

Additional machine codes used in the calculations were WANDA [15] and PDQ [16]. WANDA is a one-dimensional, few-group diffusion theory code for the IBM-704, which solves the diffusion equation with appropriate boundary conditions for a system composed of many regions in plane, spherical or cylindrical geometry, PDQ is a two-dimensional few-group diffusion theory code for the IBM-704 which can treat either X-Y or R-Z geometry. In the case of the X-Y option, there is a sufficient number of internal mesh points to represent explicitly the control rods, rod followers, and water gaps for control rod arrays in the Yankee core which have quarter-core symmetry. Both the one and two dimensional computations are performed with two groups of neutrons. It is possible to specify a transverse buckling as part of the WANDA or X-Y PDQ input so that leakage in the direction normal to the direction(s) of computation is taken into account in the neutron balance.

3.2.1 One Dimensional Calculations

One dimensional axial WANDA computations were performed when it was desired to simulate a banked movement of all control rods in the core. Radial WANDA's were used when it was desired to represent groups of fully inserted control rods.

In the one-dimensional WANDA's it was necessary to homogenize the discrete regions of the fuel assembly into either "rodded" or "unrodded" core regions depending on whether or not the assembly contained part of a control rod or a control rod follower.

A summary of group constants for the cold and hot cores is given in Appendices C, D, and E. The "homogenized" constants in Appendices C and D have been flux weighted according to a procedure described in the following section.

Axial WANDA Calculations

A series of axial WANDA's with different boron concentrations, banked control rod heights, and temperatures were run to obtain the quantitative variation of the effective multiplication factor with these three parameters. This information was then used to calculate:

(1) Variation of critical boron concentration with banked control rod height.

(2) Incremental banked control rod worth as a function of the critical position of the rods in the core.

(3) Boron worth as a function of boron concentration and banked control rod height.

(4) Moderator temperature coefficients.

In the axial WANDA's the blanket movement of control rods was accomplished by varying the position of the interface between the rodded and unrodded regions of the core. A constant radial buckling was used in all problems, the assumption being that the radial neutron leakage was independent of banked control rod height.

A flux weighting technique was used to obtain homogenized constants in the rodded and unrodded areas of the core. One dimensional unit cells comparable in geometry to a fuel assembly and containing the "fuel", water slot, and control rod (or rod follower) were defined such that the volume ratios and surface to volume ratios in the core were maintained in the cells. The WANDA code was then used to obtain region-integrated fluxes in the unit cells which, in turn, served to weight the region constants in the homogenization process.

The constants for the axial reflectors were obtained by homogenizing the steel and water into a single region and running MUFT's and SOFOCATE's, assuming a fission neutron spectrum in the reflector. The control rods extending through the upper reflector were homogenized by the "super cell" method [17].

Radial WANDA Calculations

The twenty-four control rods in the Yankee Reactor are divided into six groups of rods symmetrically located about the axis of the core. A radially symmetric arrangement of control rods is necessary to eliminate neutron flux tilting in a horizontal plane within the core. A series of radial WANDA's were run to determine the integral worth of each of the six control rod groups at the operating temperature in the reactor.

In the radial WANDA's, individual control rod groups were represented by subdividing the core into four annular regions of uniform properties and assigning each control rod group to an annulus; groups 1 and 2 to annulus 1, groups 3 and 4 to annulus 2, group 5 and 1/2 of group 6 to annulus 3, and the remaining half of group 6 to annulus 4 (see Figure 3.1). The effect of the control rods was represented by uniform fast and thermal neutron absorption cross sections added to the uniform fast and thermal unrodded cross sections of each annulus [18]. The control rod absorption cross sections were obtained by smearing the control rods over the surrounding water slot and "fuel" using the "super cell" technique, in which the neutron current into the control rod surface is converted into an equivalent poison cross section homogenized over the cell. That is, a neutron balance was used to convert a boundary leakage to a homogeneous poison [17].

Homogenized unrodded nuclear constants were taken to be the same in each annulus. A flux weighting technique, described in the previous section (Axial WANDA Calculations), was used to homogenize the constants in the "fuel", water slot, and control rod follower which make up the annuli.

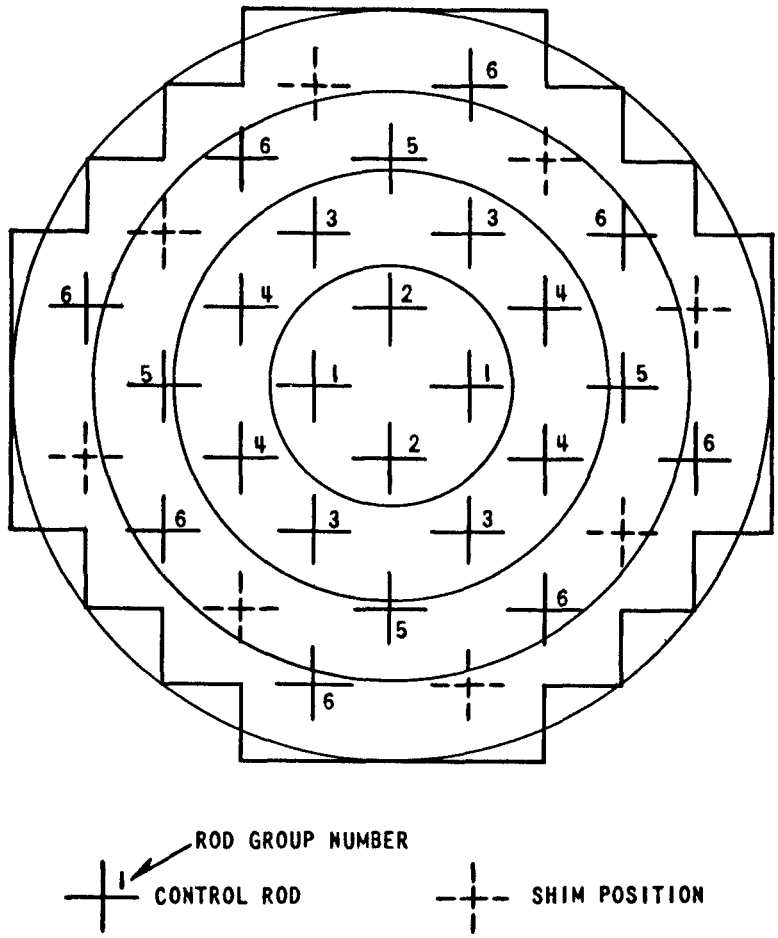

CONTROL ROD ARRAY
YANKEE ATOMIC ELECTRIC REACTOR
ROD GROUP IDENTIFICATION
AND
EQUIVALENT CORE ANNULI

FIGURE 3.1

ED. SK. 288136 C

3.2.2 Two Dimensional Calculations

Two dimensional X-Y PDQ calculations were performed primarily to determine the shutdown capability of the control rods in the core at the operating temperature.

In PDQ, the cruciform shape of the control rods and the control rod pitch may be preserved. Since the "fuel" and water slot may also be represented explicitly, no smearing of nuclear constants is required other than that used in the "fuel" of the unit cell.

A summary of group constants for the cold and hot cores is given in Appendices C and D.

3.3 Approximations

3.3.1 Non-Uniform Fuel Rod Pitch

The basic assumption of an average uniform fuel rod pitch throughout the fuel regions of the core was used in all of the nuclear calculations of the Yankee startup experiments.

The Yankee fuel assemblies were manufactured such that the fuel rod pitch along the outer row of fuel tubes was .454", with the remainder of fuel rods in the assembly at a uniform pitch of .422". This non-uniformity of fuel rod pitch over the assembly made it impossible to calculate resonance escape probabilities and thermal disadvantage factors based on a representative unit cell. In order to simplify the calculation of two group constants used in the analysis, a uniform .4256" pitch was used in all of the work.

PDQ's in X-Y geometry were run for the two types of cells. One cell was based on a uniform .4256" pitch and another with an outer region of .454" pitch and an inner region of .422" pitch.

Thermal and fast constants for the three regions of different pitch were obtained using SOFOCATE and MUFT codes. Dancoff corrections in the resonance escape probability calculations were determined for the .422" and .4256" fuel pitch regions and for the

region along the edge of the fuel assembly consisting of fuel rods with both the .422" and .454" pitch [29].

The eigenvalues from both unrodded and half-rodded cell PDQ's with the actual combination of fuel rod pitches and the average fuel rod pitch were compared. In the unrodded cell, the average .4256" pitch approximation led to an underestimate in k_{eff} of .043%. In the half rodded cell the approximation resulted in an overestimate in k_{eff} of .067%. Both differences represent relatively small effects on reactivity.

3.3.2 Blanket Control Rod Representation

The axial WANDA problems described in Section 3.2.1 took into account the neutron flux disadvantage factor for the control rod followers and adjacent water slot, but included two basic assumptions concerning control rods:

(a) The cruciform absorber may be represented geometrically by a one dimensional absorber; i.e., the assumption was made that the loss in neutron absorption at the inside corner of the cruciform is offset by the increased absorption at the tips.

(b) The control rods are uniformly distributed in the core. (The rods are actually preferentially located toward the center of the core.)

A study was conducted utilizing cell PDQ and WANDA calculations at operating temperature to evaluate the first approximation. It was found that the effect of the estimated thermal absorption cross sections in the control rod [28] and the one dimensional approximation in WANDA resulted in an underestimate of cell reactivity of about 1% ($\Delta k/k$) or an overestimate in control rod worth of 7% for a fully rodded cell.

A quantitative estimate of the second approximation at the operating temperature of the core was obtained from a comparison between corresponding full core axial WANDA and XY-PDQ calculations

combined with the evaluation of the first approximation. The results indicate that control rods uniformly distributed in the core are worth 29% less than the actual configuration which has a greater concentration of control rods in the high neutron importance region toward the center of the core. The axial WANDA's were therefore conservative in their estimate of the shutdown capability of the control rods in the reactor at the operating temperature in the core.

The effect of the two approximations taken together is a 22% underestimate of control rod worth in the axial WANDA problems. This represents an overestimate in the fully rodded core reactivity of 3.2% at the operating temperatures.

3.3.3 Constant Radial Reflector Savings

In all axial WANDA computer problems the radial buckling was based on a reflector savings of 8.0 cm [1]. No consideration was given to a possible variation of the reflector savings of the core with temperature, boron concentration, or control rod configuration. However, it has been shown experimentally that the radial reflector savings is relatively independent of boron concentration [1]. Also, the reflector savings used in the calculations is midway between the value measured at ambient temperature and the value expected at operating temperature. In addition, it may be shown that a deviation from the above radial reflector savings by as much as 1 cm represents only a 0.05% change in the multiplication factor of the core. Since a more significant departure than this from the value used in the calculations would not be anticipated, the reflector savings, and thus the radial buckling of the core, are assumed independent of these three variables for one dimensional axial calculations.

4.0 REACTOR CHARACTERISTICS AT AMBIENT TEMPERATURE

This section summarizes the results of reactivity calculations performed for the Yankee reactor at ambient temperature (100°F). In addition to the nuclear parameters of interest from the design standpoint, critical boron concentrations and incremental banked control rod worths were calculated for comparison with data to be obtained in the nuclear startup experiments. Since detailed control rod group worth information is not required in the cold reactor, only one dimensional calculations were performed for banked control rods. Inherent in this procedure is the underestimate of total control rod worth discussed in the previous section.

A table of pertinent nuclear design data at ambient temperature is included in Section 7.0.

4.1 Core Reactivity

The Yankee reactor has a cold, unrodded multiplication factor of 1.167. The excess multiplication must be provided in the cold, clean core to maintain criticality at operating temperature for the desired core lifetime. Specifically, the relatively large negative temperature coefficients (moderator plus Doppler), fuel burnup, and equilibrium xenon and samarium poisoning dictate the amount of reactivity required in the core above that needed for criticality in the cold, clean condition. Control of the Yankee reactor is provided by a combination of control rods and a chemical neutron absorber dissolved in the coolant-moderator (boric acid). Complete control by control rods alone would involve a larger number of control rods, precision drive mechanisms and penetrations in the pressure vessel head, in addition to subdividing the fuel assemblies. The greater number of penetrations in the vessel head would complicate fabrication and introduce uncertainty in the structural integrity of the vessel. The twenty-four movable control rods are used to control reactivity at operating temperatures. Boric acid is added for intermediate temperature range shutdown and to render the core subcritical in a clean condition at room temperature.

Table 4.1 contains the results of axial WANDA calculations of k_{eff} for various combinations of boron and control rod poisoning for the

Table 4.1

COLD MULTIPLICATION FACTORS FOR VARIOUS CORE CONDITIONS

No Control Rods - No Boron	1.167
Fully Rodded - No Boron	1.043
Fully Rodded - 560 ppm Boron	1.000
Fully Rodded - 1275 ppm Boron	0.950
Fully Rodded - 1600 ppm Boron	0.929

core at ambient temperature. Since the above calculations assumed a uniform radial distribution of control rods, the k_{eff}'s in the table are somewhat high (Section 3.3.2). With the actual radial control rod distribution, for example, 1275 ppm boron will render the core subcritical by more than 5% (Δk_{eff}) indicated in the table.

4.2 Boron Concentration Vs. Banked Control Rod Position

The WANDA computer program was used to study the interdependence of the concentration of boron in the critical core and the banked movement of control rods. The axial position of the interface between the rodded and unrodded regions in the core, at each of several boron concentrations, was varied to represent banked control rod movement in an effort to bracket a critical multiplication factor. At each of the chosen boron concentrations, then, a banked control rod height corresponding to a critical reactor was obtained. The results of the calculations are plotted in Figure 4.1. The slope of the curve in Figure 4.1 and consequently the worth of the control rod is the greatest between banked rod heights of 10 and 20 inches. This is due to a shift in power to the lower, unrodded core, which occurs in this interval of control rod withdrawal, such that the region of maximum power density is located between 10 and 20 inches from the bottom of the core.

4.3 Boron Worth

The WANDA results from Section 4.1 were also utilized in determining the boron worth in the core. At each of several banked control rod heights, values of k_{eff} from a series of WANDA's corresponding to a range

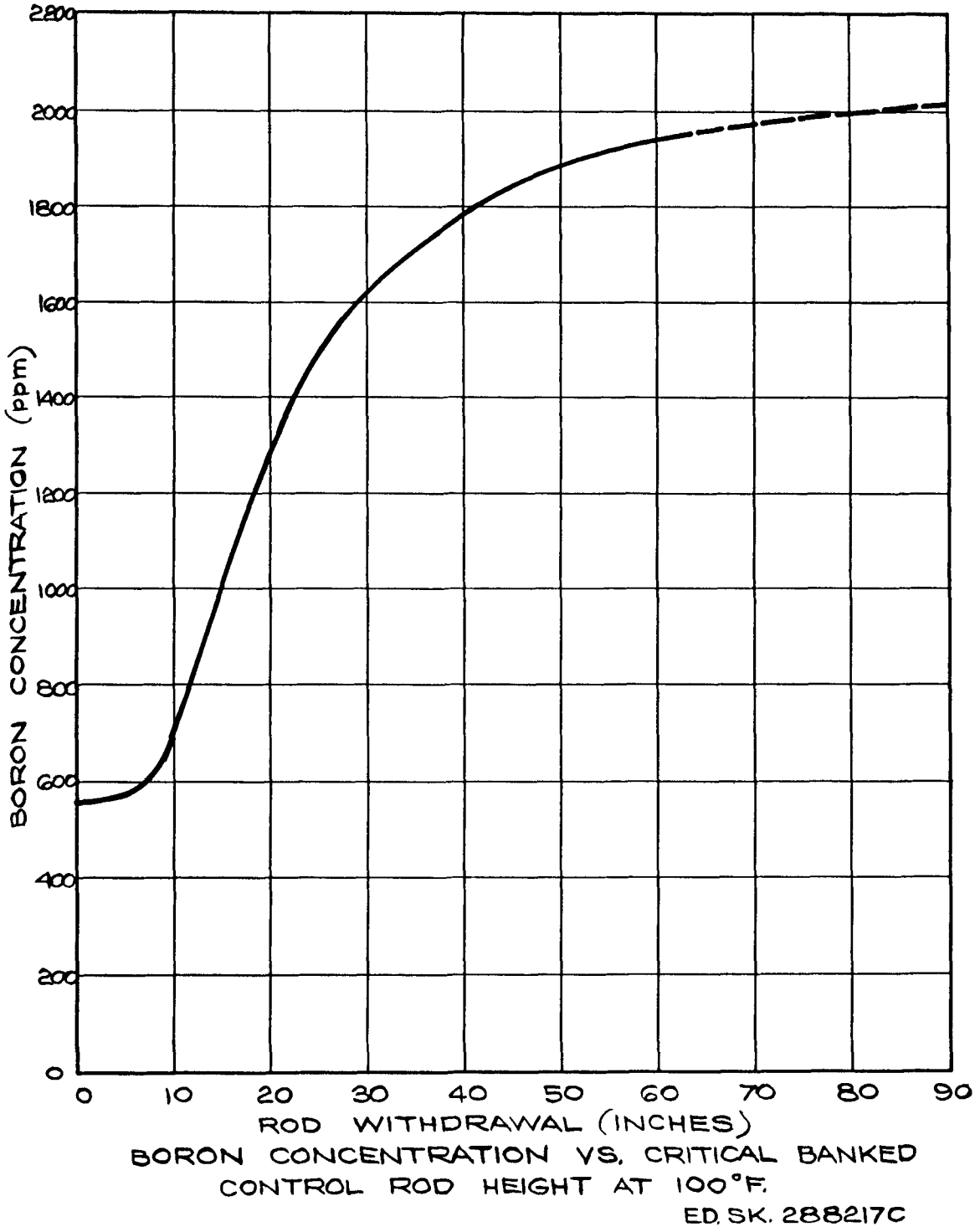
BORON CONCENTRATION (ppm)
2200
2000
1800
1600
1400
1200
1000
800
600
400
200
0
0
10
20
30
40
50
60
70
80
90
ROD WITHDRAWAL (INCHES)
BORON CONCENTRATION VS. CRITICAL BANKED CONTROL ROD HEIGHT AT 100°F.
ED. SK. 288217C

Figure 4.1

in boron concentration of 0 to 1900 ppm were used to obtain values of $1/k\ \partial k/\partial C_B$ (approximated by the expression, $1/k_{average}\ \Delta k/\Delta C_B$). The $1/k\ \partial k/\partial C_B$'s at the critical boron concentration for control rod heights from 0 to 40 inches are plotted in Figure 4.2. Values of $1/k_\infty\ \Delta k_\infty/\Delta C_B$ for the completely rodded and unrodded cores were also calculated and plotted in the figure. At control rod heights greater than 20 inches, the boron worths in the critical core are essentially the same as those in a completely unrodded core because at these extended rod heights the power density (and neutron importance) is greatest in the unrodded core. Leakage effects on boron worth are very small, since boron has little effect on the neutron slowing down length. For control rod heights below 10 inches, the boron worth in the critical core approaches that in a completely rodded core, also illustrated in Figure 4.2.

4.4 Banked Control Rod Worth

The results of the WANDA problems in Section 4.1 were also used to determine the change in $1/k\ \partial k/\partial h$ with banked control rod height in a critical core. To obtain the variation of $1/k\ \partial k/\partial h$ with h (banked control rod height), a histogram was developed in which $1/k\ \partial k/\partial h$ was assumed to be constant at a value equal to $1/k\ \Delta k/(h_1-h_2)$ in the region between h_1 and h_2, for boron concentrations very close to $k_{eff} = 1$. A curve was then superimposed on the histogram to represent a more precise estimate of the variation of $1/k\ \partial k/\partial h$ with control rod withdrawal. The histogram and curve are plotted in Figure 4.3. The curve has a peak at a rod height of approximately 12.5 inches. In the vicinity of 12.5 inches the peak power shifts from the lower to the upper core region. When this shift is completed, a rapid reduction in $1/k\ \partial k/\partial h$ occurs.

At extended control rod heights it would be expected that the reactor would behave like a single region unrodded core. This was found to be true, in that $1/k\ \partial k/\partial h$ varied with the inverse cube of control rod height as would be predicted from a single region expression for the multiplication factor, accounting for the rodded core by a constant reflector savings.

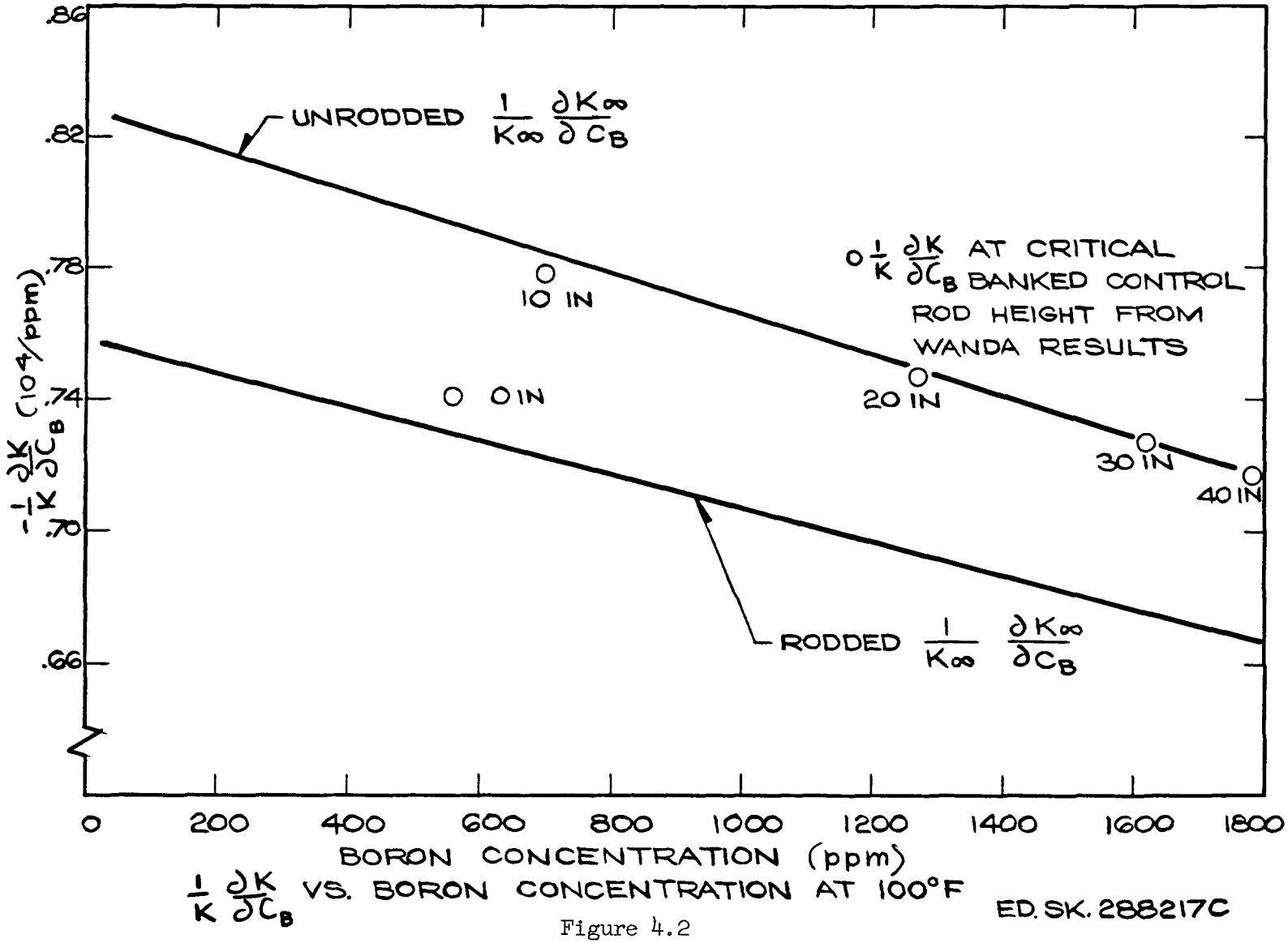
.86
.82
.78
.74
.70
.66
$-\frac{1}{K}\frac{\partial K}{\partial C_B}$ (10⁴/ppm)
UNRODDED $\frac{1}{K\infty}\frac{\partial K\infty}{\partial C_B}$
10 IN
0 IN
$\frac{1}{K}\frac{\partial K}{\partial C_B}$ AT CRITICAL BANKED CONTROL ROD HEIGHT FROM WANDA RESULTS
20 IN
30 IN
40 IN
RODDED $\frac{1}{K\infty}\frac{\partial K\infty}{\partial C_B}$
0
200
400
600
800
1000
1200
1400
1600
1800
BORON CONCENTRATION (ppm)
$\frac{1}{K}\frac{\partial K}{\partial C_B}$ VS. BORON CONCENTRATION AT 100°F
ED. SK. 288217C

Figure 4.2

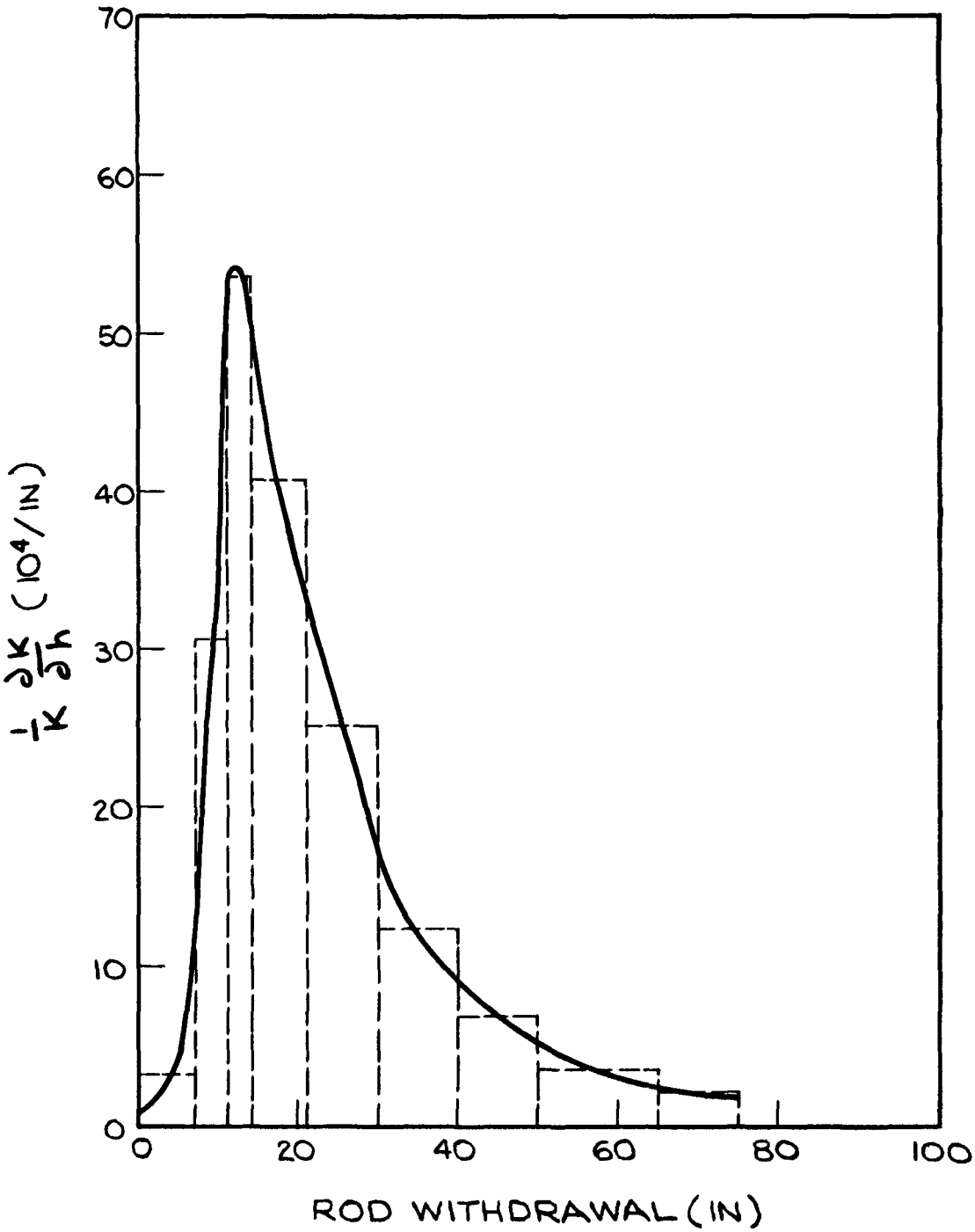

$\frac{1}{K}\frac{\partial K}{\partial h}$ VS. CRITICAL BANKED CONTROL ROD HEIGHT AT 100° F

E.D. SK.288216-C

Figure 4.3

A series of multiplication factors for the completely rodded and unrodded cores were calculated at various boron concentrations. The ratio of rod worths in the borated core to the worth in a clean core are plotted in Figure 4.4*. The worth of the control rods will decrease with increasing boron concentration, according to the figure, because of the competition for thermal neutrons afforded by the boron.

---

* Rod worth was defined in terms of a reduction factor, R, where R = ratio of the multiplication factors in the rodded core to the unrodded core.

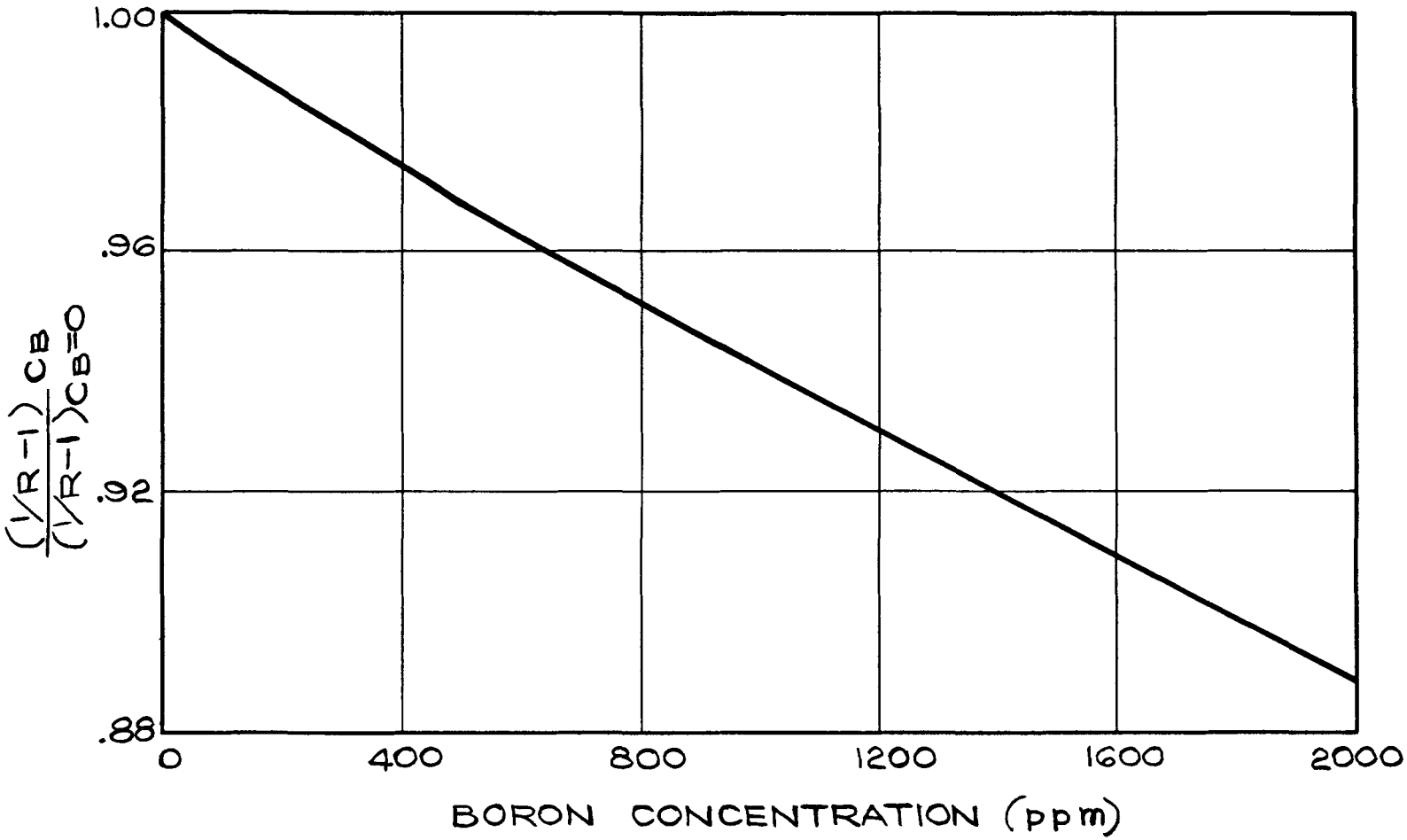

EFFECT OF BORON CONCENTRATION ON CONTROL ROD WORTH AT 100°F. ED.SK. 288218C

Figure 4.4

5.0 REACTOR CHARACTERISTICS AT OPERATING TEMPERATURE

The nuclear characteristics at operating temperature of the core are extremely important from the standpoint of operation, and have therefore been subjected to a more detailed analysis than the cold characteristics. Control rod group worths for the reference control rod withdrawal sequence have been evaluated using both one and two dimensional techniques. These worths are valuable in estimating control rod movements required to compensate for various reactivity effects. They also yield values for the total rod worth and the hot clean shutdown capability of the control rods. The change in reactivity associated with xenon and samarium poisoning, and the Doppler effect on resonance absorption in U-238 have also been studied for various power levels and control rod configurations. These characteristics depend on the control rod distribution because of the effect of control rods on power distribution and neutron importance weighting function. In addition to the above parameters, both boron worth and banked control rod worth were studied in order to provide calculations which could be compared to data obtained during the startup experiments.

5.1 Core Reactivity Effects

Since the Yankee core has a negative temperature coefficient of reactivity, the effective multiplication factor of the hot core is less than that of the core at ambient temperature. Table 5.1 contains calculated values of k_{eff} for various combinations of boron and control rod poisoning.

Table 5.1

HOT (0 POWER) MULTIPLICATION FACTORS AND REACTIVITY SWINGS FOR VARIOUS CORE CONDITIONS

	k_{eff}	Reactivity Swing* (%)
No Control Rods - No Boron	1.113	-4.8
No Control Rods - 1750 ppm Boron	1.000	-2.0
Fully Rodded - No Boron	.942	-7.4

* Reactivity changes are expressed in terms of (1/R - 1), where $R = k_{final}/k_{initial}$.

The unrodded values of k_{eff} quoted in the table are based on one dimensional calculations. The fully rodded multiplication factor given in the table is the result of a full core X-Y PDQ calculation. It indicates that the design objective for the first core of providing sufficient control with 24 control rods to render the unborated core at the operating temperature and zero power 3% subcritical will be met. It is of interest to compare these values with those at ambient temperature to evaluate the cold-to-hot reactivity swing. Table 5.1 also gives the reactivity difference between ambient and operating temperatures for three core conditions. These values illustrate the effect of temperature on control rod worth and boron worth, as well as reactivity. During reactor startup, reactivity control will be maintained by some combination of control rods and boric acid, so that the reactivity swing will be somewhere between the limits given in Table 5.1.

5.2 Boron Concentration Vs. Banked Control Rod Position

The WANDA computer program was used to study the effect of boron concentration on the banked control rod position in the critical core at the operating temperature (514°F). A series of computer problems analogous to those at the ambient temperature were run with a maximum boron concentration of 1080 ppm. To determine the critical banked control rod height at boron concentrations above 1080 ppm, the results of the axial WANDA's were graphically extrapolated as illustrated by Figure 5.2. At a banked rod position of 50 inches, for example, the critical boron concentration was taken to be 1490 ppm. The complete variation of boron concentration with banked control rod height in the critical reactor is summarized in Figure 5.1.

5.3 Boron Worth

The results of the WANDA calculations of Section 5.2 were used to determine the boron worth in the core at the operating temperature. The procedure described in Section 4.3 was followed in calculating values of $1/k_{\infty}\ \Delta k_{\infty}/\Delta C_B$ in the fully rodded and unrodded cores and $1/k\ \partial k/\partial C_B$ in the critical core. The results are plotted in Figure 5.3. Here, as at ambient temperature, it will be observed that for banked control rod

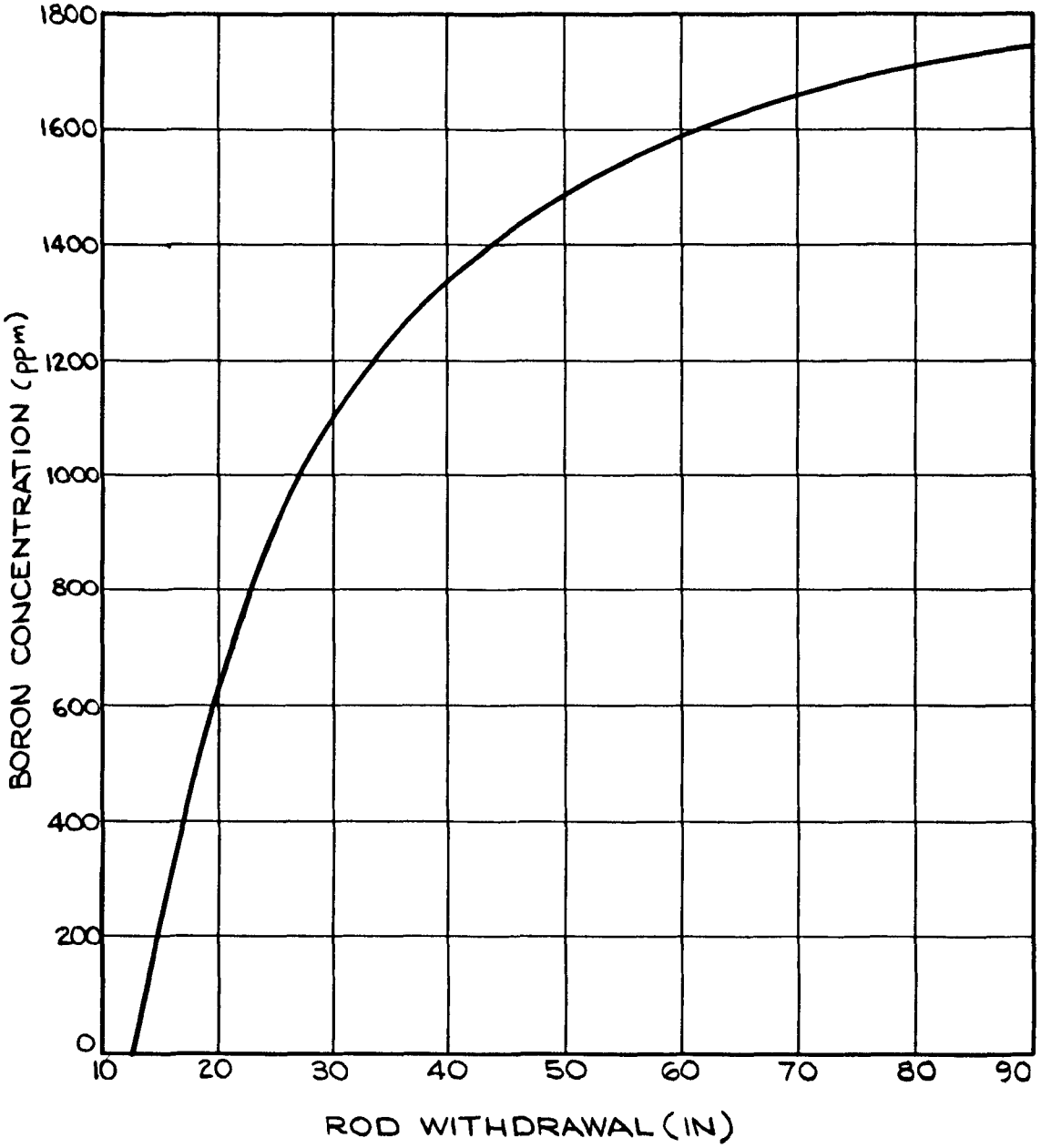

BORON CONCENTRATION VS. CRITICAL BANKED CONTROL ROD HEIGHT AT 514° F

Figure 5.1

S.D. SK. 288215-C

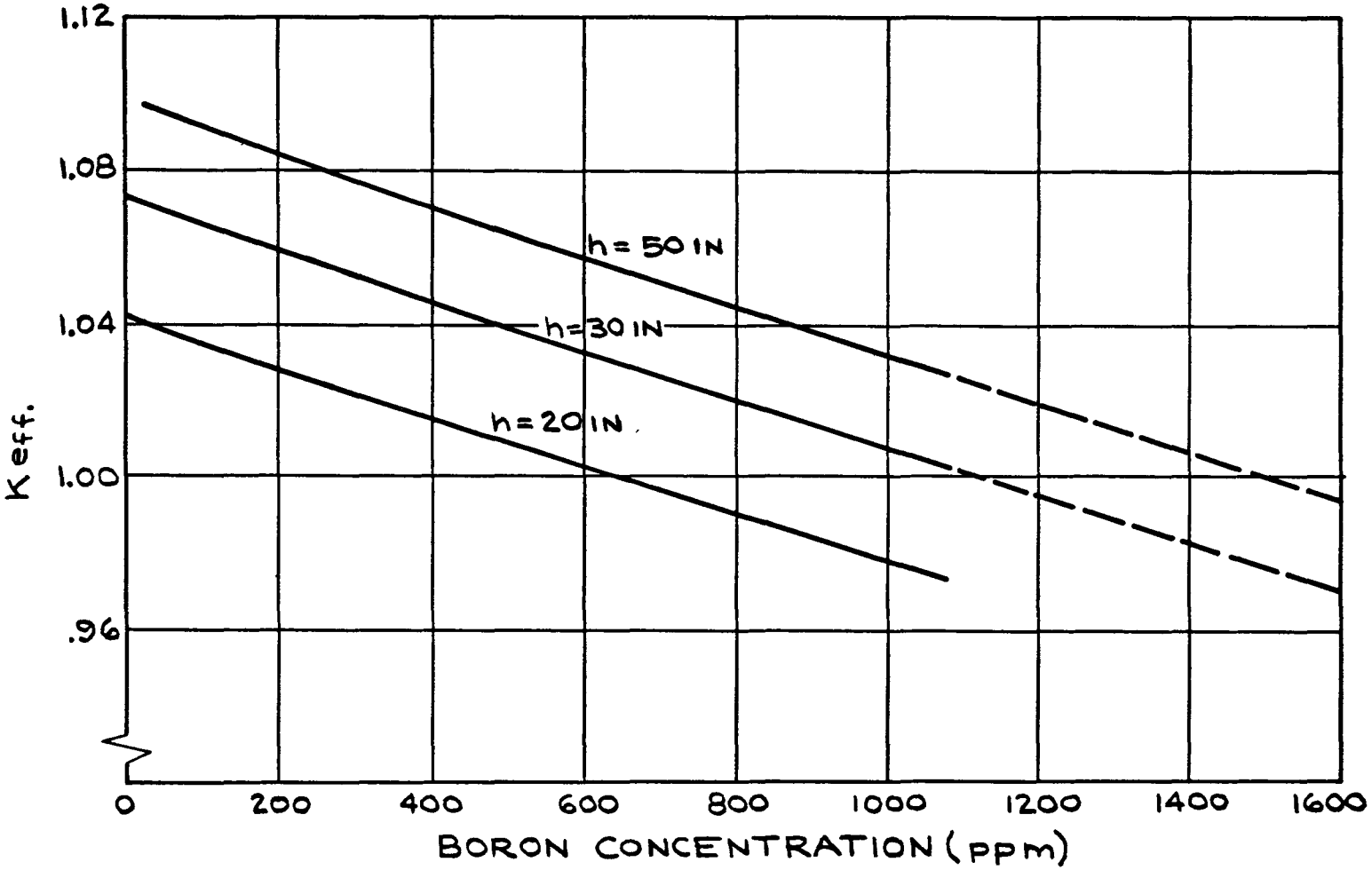

Keff. vs. BORON CONCENTRATION FOR VARIOUS BANKED CONTROL ROD HEIGHTS AT 514° F

Figure 5.2

ED
SK 288221C

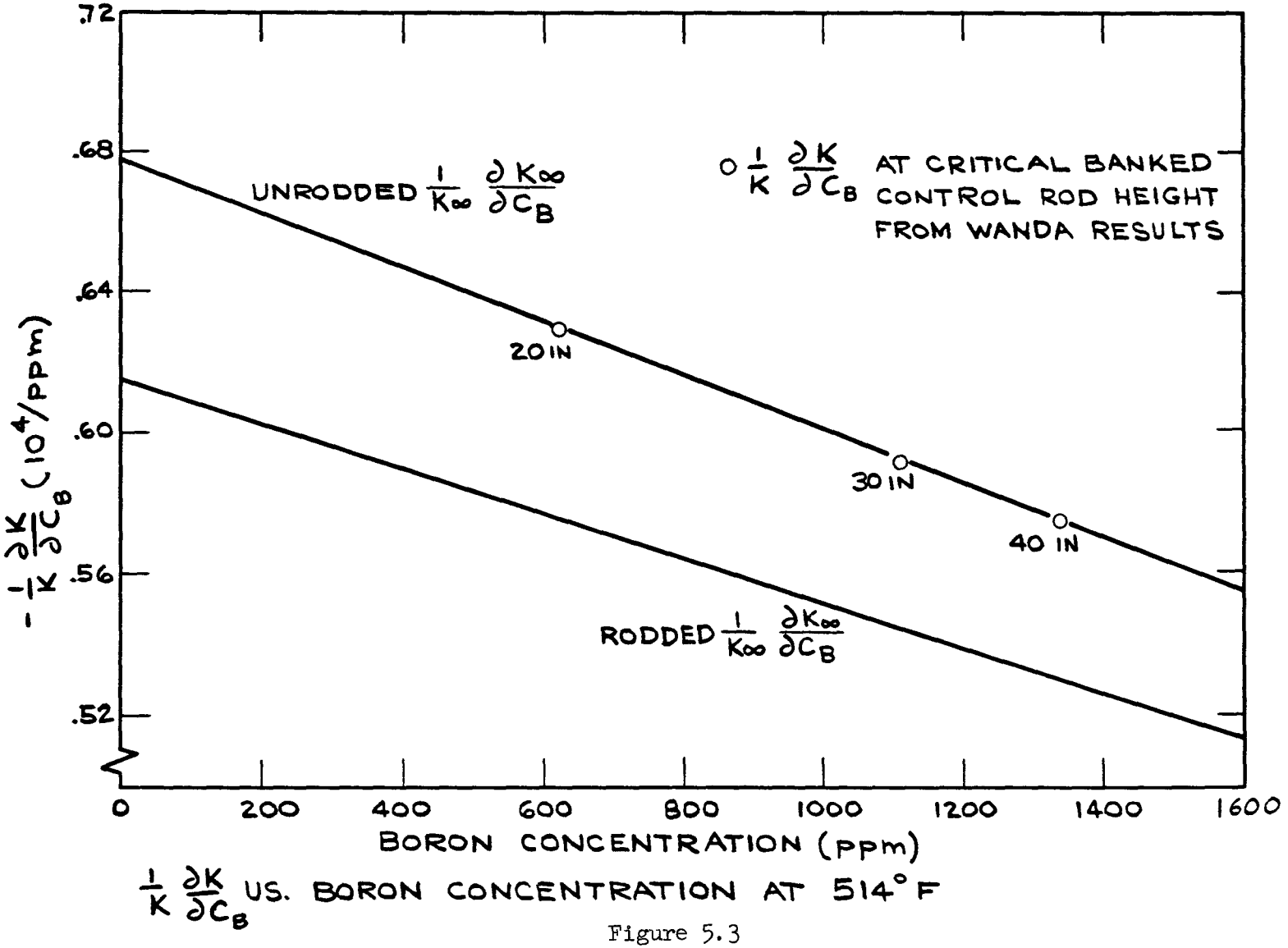

Figure 5.3

ED SK 288 222C

heights greater than 20 inches the boron worths in the critical core are equal to those in a fully unrodded core. Comparing Figure 4.2 with Figure 5.3, it appears that the boron worth in the core at the ambient temperature is greater than the worth at the operating temperature. This is due to the fact that there is less water, by weight, in the hot core than in the cold, and therefore less boron at a constant value of "parts-per-million" in the hot core. That is, the macroscopic absorption cross section of boron decreases, with increasing temperature, at a greater rate than the cross section of the core.

5.4 Banked Control Rod Worth

The results of the axial WANDA problems in Section 5.2 were used in a procedure identical to the one in Section 4.4 to obtain the effect of the banked control rod position in the core on $1/k\ \partial k/\partial h$. The same general conclusions which were drawn at the ambient temperature may also be drawn about Figure 5.4. Between control rod heights of 0 and 12.5 inches, the curve has been dotted to indicate that the reactor is subcritical. It is fairly obvious in comparing Figure 4.3 with Figure 5.4 that the control rods are worth more in the core at the operating temperatures. This is due to the fact that the neutron migration area in the hot core is greater than in the cold because of the decreased density of the moderator. The neutrons travel farther from their point of origin in the fuel in the process of thermalization in the hot core and, therefore, the effective "range" of the control rods as a neutron sink in the core becomes enlarged. The variation of rod worth with temperature is essentially linear up to a temperature of approximately 470°F. At higher temperatures, the density of the water decreases more rapidly and rod worth increases with temperature at a greater rate than below 470°F. Based on axial WANDA calculations, the total rod worth at 100°F is 11.9%, where worth has been defined in terms of a reduction factor according to Section 5.5. At 470°F, the worth is 14.2% and increases to 14.8% at 530°F.

At operating temperature, control rod worth is also dependent on the boron content of the core. The result of calculations similar to those which were completed at the ambient temperature are plotted in

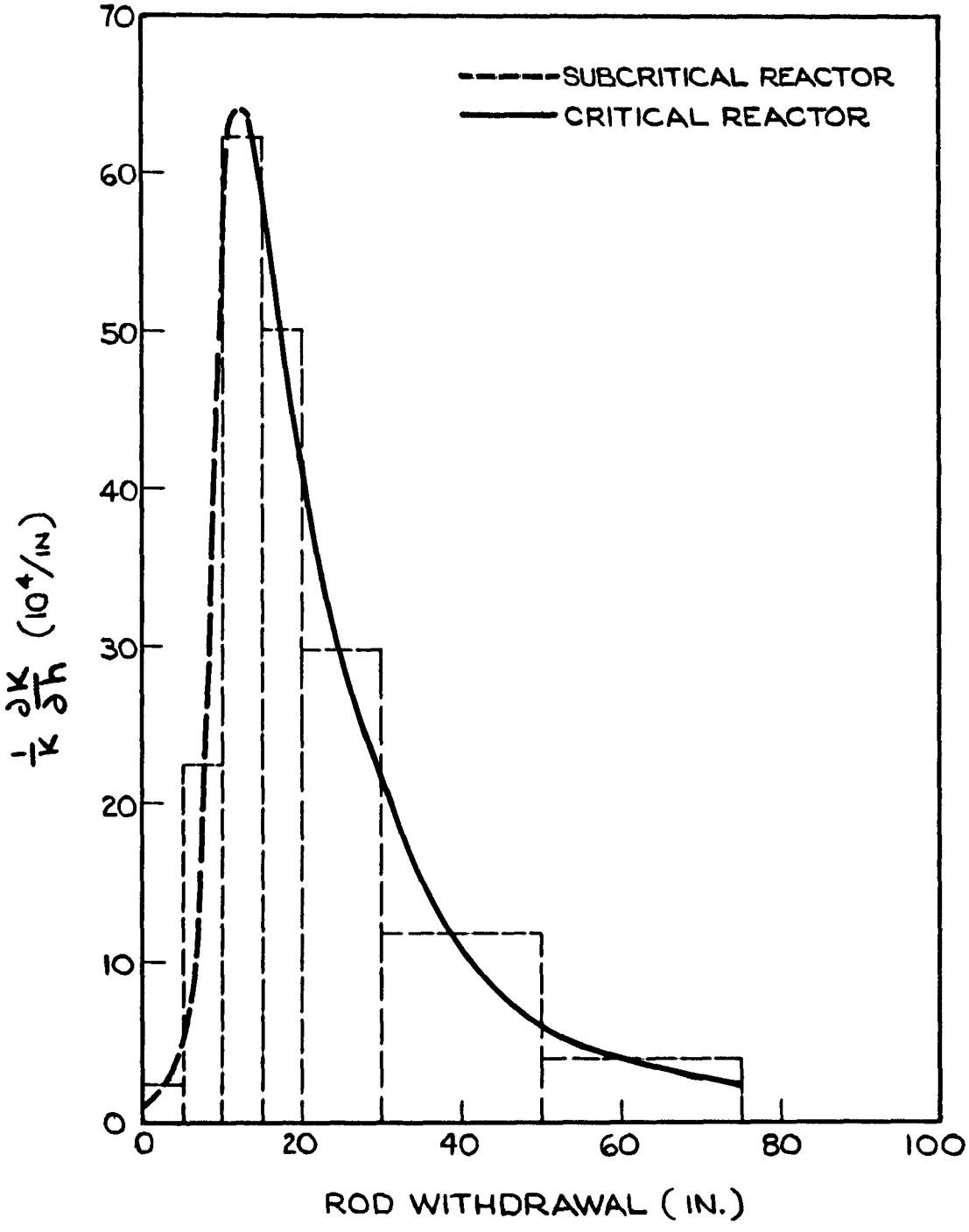

$\frac{1}{K}\frac{\partial K}{\partial h}$ VS. CRITICAL BANKED CONTROL ROD HEIGHT AT 514° F

Figure 5.4

E.D. SK: 288216-C

206 042

Figure 5.5. Comparing this figure with Figure 4.4 it would appear that the boron is worth more in the core at the ambient temperature than at the operating temperature; that is, the boron seems to have a greater effect on control rod worth in the cold core, confirming the results of Section 5.3.

5.5 Control Rod Group Worth

Control rod worth was defined in terms of effective core multiplication factors according to the expression below:

$$\text{Control Rod Worth} = (1/R - 1),$$

where

$$R = k_{\text{with rods}}/k_{\text{without rods}}.$$

Both WANDA and PDQ computer programs were used to obtain the required multiplication factors. Table 5.2 summarizes the results of the calculations.

It will be noticed in the table that the worth of a control rod group in a particular rod array was obtained. (See Figure 3.1 for identification of control rod groups in the core.) The worth of a control rod group is effected by the presence of other control rods. For example, the worth of one of the outer rod groups, such as group 6 will be greater with an inner group present than without. The inner control rods would tend to increase the flux around the outer edge of the core such that group 6 would be in a relatively high neutron importance area. The sequence of arrays was therefore chosen to correspond to the control rod withdrawal program which will be followed during the lifetime of the core. Only the worth of completely inserted control rods was obtained. The worth of partially inserted rods was calculated only for the blanket movement of all rod groups already discussed in Section 5.4.

Examination of Table 5.2A indicates good agreement between one and two dimensional calculations for large numbers of control rods. Since the PDQ calculation is a more accurate representation of the core geometry, it is expected to yield more reliable rod worths. WANDA, which represents control rods with a uniform absorption cross section smeared over a large

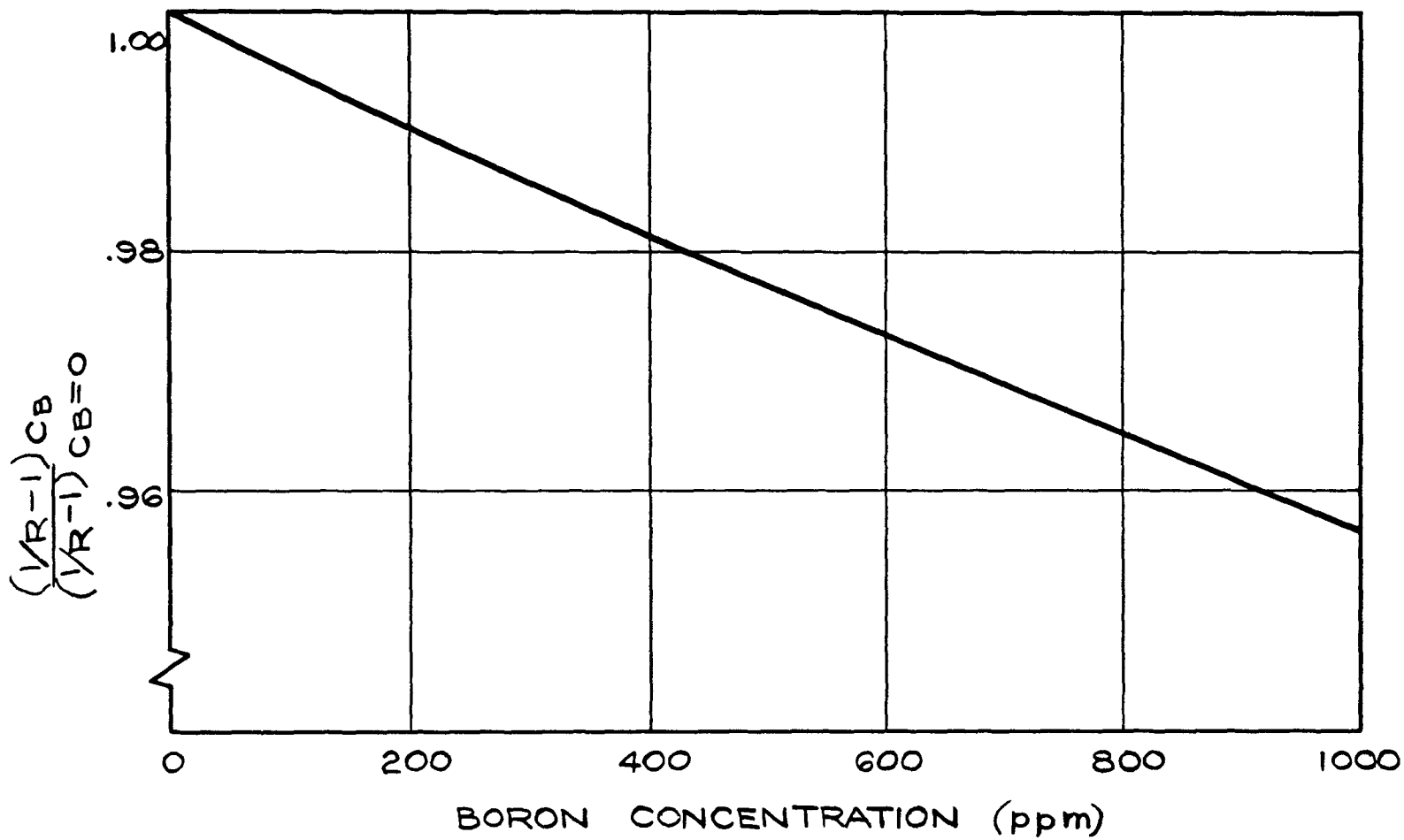

EFFECT OF BORON CONCENTRATION ON CONTROL ROD WORTH AT 514°F. ED.SK.288218C

Figure 5.5

Table 5.2-A

REACTIVITY WORTH OF SEVERAL CONTROL ROD GROUP PATTERNS AT 514°F

Rod Pattern	k_{eff}		Reactivity Worth (%)	
	WANDA	PDQ	WANDA	PDQ*
0	1.113	---	---	---
1	1.091	---	2.1	---
51	1.065	1.067	4.6	4.3
351	1.025	1.033	8.6	7.7
2351	1.015	1.025	9.7	8.6
42351	0.994	0.999	12.0	11.4
642351	0.943	0.942	18.1	18 2

Table 5.2-B

REACTIVITY WORTH OF CONTROL ROD GROUPS IN THE REFERENCE CONTROL ROD WITHDRAWAL SEQUENCE AT 514°F (6-4-2-3-5-1)

Rod Group	Reactivity Worth	
	WANDA	PDQ
6	6.1	6.8
4	2.3	2.8
2	1.1	0.9
3	4.0	3.4
5	2.5	---
1	2.1	---

* Based on the WANDA unrodded k_{eff} (1.113).

radial region, is not capable of representing aximuthal flux variations, and will be in error in determining reactivity differences involved in insertion of a small number of control rods which do not have aximuthal symmetry.

5.6 Steady State Doppler and Fission Product Poisoning Effects

In the core at operating temperature during power operation, there are two important effects which influence reactivity. The first is a fuel temperature effect. At elevated fuel temperatures, resonance absorption in U-238 increases due to the Doppler broadening of neutron capture resonances. The second is a poison effect caused by the build-up of Xe-135 and Sm-149 - decay products of the two fission products Te-135 and Nd-149, respectively.

The WANDA computer code was used to calculate the reduction in reactivity due to the Doppler effect, Xe-135 and Sm-149, and a combination of both at half and full power. The Doppler effect was represented by adding a fast absorption cross section, $\Delta\Sigma_{af}$, to the zero power fast absorption in the form,

$$\Delta\Sigma_{af_R} = \frac{\Delta p\ \alpha_p\ (P_R/P_{avg})}{\Delta p\ \alpha_p\ (P_R/P_{avg}) + 1} (\Sigma_{af} + \Sigma_r + D_f B^2) \text{(See Appendix B).} \quad (5.1)$$

Where, the subscript "R" refers to a particular region in the radial WANDA, and,

Δp = fractional power (100 at full power).

αp = power coefficient per % power (See Section 6.2).

$\frac{P_R}{P_{avg}}$ = ratio of power in a region to the average power in the core.

Σ_{af}* = fast absorption cross section of the core at zero power (cm^{-1}).

Σ_r* = core removal cross section (cm^{-1}).

D_f* = core fast diffusion coefficient (cm).

B^2 = core geometric buckling (0.000701 cm^{-2}).

---

* See Appendix D.

The xenon poisoning was represented by adding a thermal absorption cross section, $\Sigma_{a,Xe}$, to the clean thermal absorption in the form:

$$\Sigma_{a_{Xe_R}} = \frac{y_{Xe}\,(\varphi\Sigma_f)_{avg}\,(P_R/P_{avg})}{\frac{\lambda_{Xe}}{\sigma_{Xe}} + \varphi_{2_{avg}}\,(\varphi_{2R}/\varphi_{2_{avg}})} \quad \text{(See Appendix B)} \qquad (5.2$$

where,

y_{Xe} = yield of Xe-135 per fission (.064).

$(\varphi\Sigma_f)_{avg}$ = $(\varphi_2\,\Sigma_{f2} + \varphi_1\,\Sigma_{f1})_{avg}$ = sum of fast and thermal fission reaction rates (1.83×10^{12} cm^{-3} sec^{-1}).

λ_{Xe} = decay constant for X3-135 (2.11×10^{-5} sec^{-1}).

σ_{Xe} = microscopic absorption cross of Xe (1.44×10^{-18} cm^2).

$\varphi_{2_{avg}}$ = average core thermal flux (1.9×10^{13} cm^{-2} sec^{-1}).

$(\varphi_{2R}/\varphi_{2_{avg}})$ = ratio of thermal flux in a region to the average core thermal flux.

Sm was assumed to be uniformly distributed. The thermal Sm cross section was obtained from:

$$\Sigma_{a_{Sm}} = \frac{y_{Sm}\,(\varphi\Sigma_f)_{avg}}{\varphi_{2_{avg}}} \text{ (See Appendix B)}, \qquad (5.3)$$

where,

y_{Sm} = yield of Sm-149 per fission (0.0115).

The concept of a reduction factor was utilized to determine the worth of the Xe and Sm and the Doppler effect. Here the reduction factor was defined as:

$$R = \frac{k\ (\text{Xe and Sm and/or Doppler})}{k\ (\text{clean, zero power})}$$

Assuming the power in the core to be uniformly distributed ($P_R/P_{avg} = 1$) and neglecting the effect of fuel depletion and plutonium build-up, the worths of xenon and samarium poisoning and Doppler broadening in the fuel, as calculated by WANDA, are plotted in Figure 5.6.

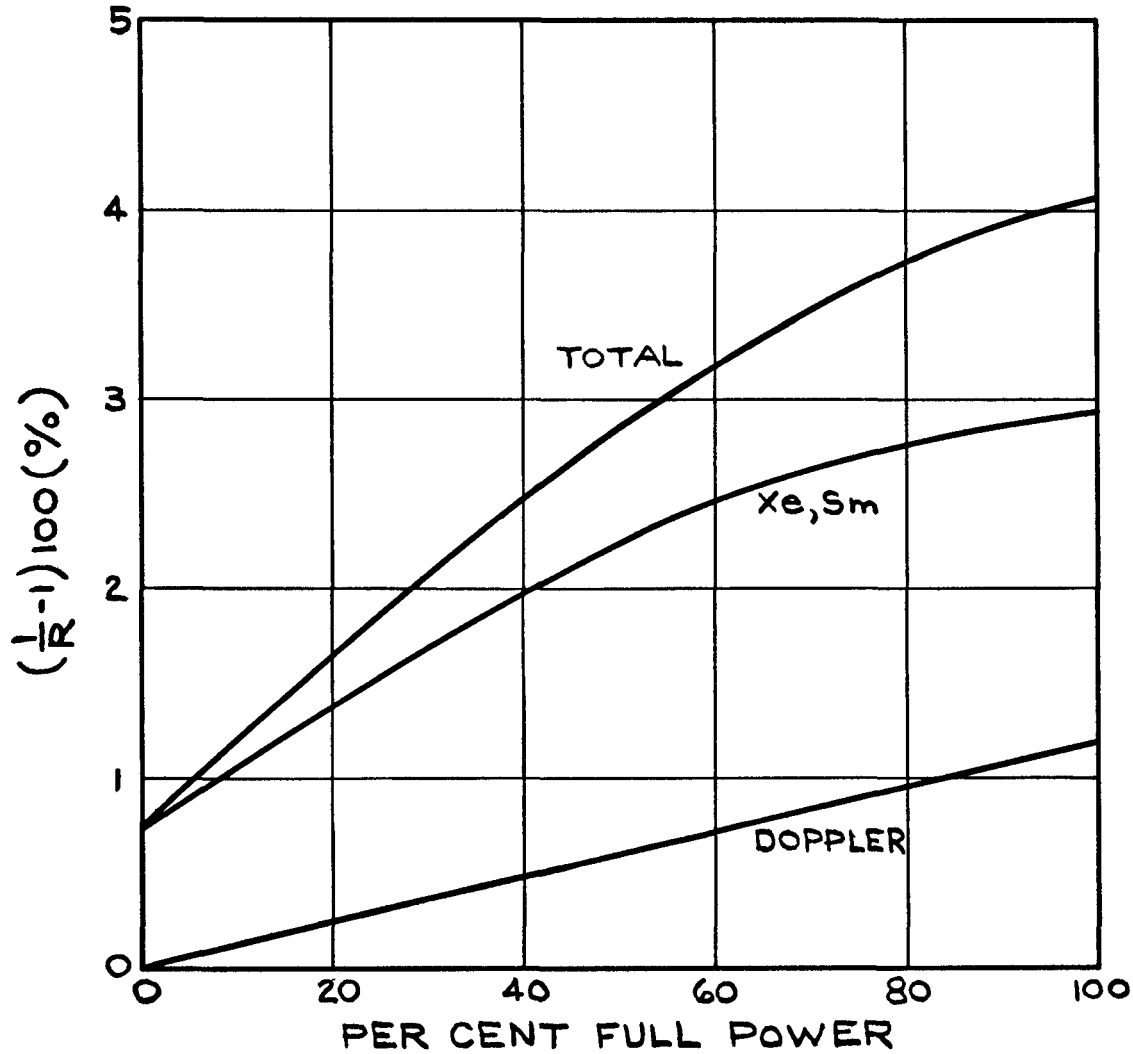

WORTH OF DOPPLER EFFECT IN FUEL, EQUILIBRIUM XENON AND SAMARIUM POISONING, AS A FUNCTION OF UNIFORMLY DISTRIBUTED POWER

Figure 5.6

ED SK 288222c

Statistical weight factors which may be applied to Figure 5.6 were also calculated to account for non-uniform power distributions in the core. The variation of xenon poisoning and Doppler broadening with power was taken into account in the radial WANDA's by inserting values of $\Delta\Sigma_{af_R}$ and $\Sigma_{A_{Xe_R}}$ based on the corresponding values of P_R/P_{avg} in each radial region. Four radial regions were used in WANDA calculations as illustrated in Figure 3.1. For various control rod configurations the worths calculated for the non-uniform power distribution were divided by the corresponding worths assuming a uniform power distribution. These so-called "statistical weight factors" were calculated at half and full power and are tabulated below.

Table 5.3

STATISTICAL WEIGHT FACTORS FOR NON-UNIFORM DOPPLER AND XENON EFFECTS

Rod Arrays	$K_{Doppler}$		K_{Xe}		K_{total}	
	50%*	100%	50%	100%	50%	100%
0	1.95	1.95	1.19	1.16	1.34	1.32
1	1.54	1.54	1.11	1.10	1.19	1.18
351	1.27	1.27	1.03	1.03	1.06	1.06
42351	1.39	1.39	1.04	1.04	1.09	1.09

* % of full power

Contributing to the shutdown of the core near the beginning of life should it be necessary to render the core subcritical, would be the build-up of any Samarium-149. Samarium-149 is stable and represents a negative contribution to reactivity throughout the lifetime of the core. Xenon-135, of course, also has a poisoning effect on reactivity, but, because of decay, would not be effective after a prolonged shutdown.

The combination of equilibrium xenon and samarium represents approximately 3% in excess multiplication. Samarium makes up about one-fourth of this amount or 0.7% in excess k_{eff}.

6.0 KINETICS CHARACTERISTICS

Two very important characteristics of the pressurized light water reactor are its large negative moderator temperature coefficient and its negative Doppler coefficient. The large moderator temperature coefficient is a result of the rapid rate of change in H_2O density with temperature for pressurized H_2O at elevated temperatures, while the negative Doppler coefficient is a result of the broadening of neutron capture resonances as the fuel temperature increases. The moderator temperature coefficient contributes to the overall stability of the plant and is important in the control of slow transients and power changes. The Doppler coefficient contributes to the stability of the reactor in the event of rapid changes in reactivity and power level. In this section, the moderator temperature coefficient, Doppler and power coefficients, pressure and void coefficients, and the prompt neutron lifetime and effective delayed neutron fraction are obtained. In all cases, the coefficients have been calculated for a just critical core. That is, a core with such a combination of control rods and boric acid dissolved in the moderator as to make $k_{eff} = 1$.

6.1 Moderator Temperature Coefficient

This coefficient is associated with changes in moderator temperature. It is a slow coefficient, compared to the fast Doppler coefficient associated with changes in fuel temperature. A change in the fission rate results in an immediate change in fuel temperature, but there is a time constant of the order of 10 seconds for the transfer of heat from the fuel to the moderator. The temperature coefficient will be defined as the fractional change in effective multiplication factor per degree change in moderator temperature.

$$\alpha_T = \frac{1}{k_{eff}} \frac{\partial k_{eff}}{\partial T}. \qquad (6.1)$$

The temperature coefficient was obtained by calculating k_{eff} as a function of temperature and taking the slope of the curve of k_{eff} against temperature. The coefficient was calculated at three moderator temperatures and for various boron concentrations. The reactor was made critical at each

temperature and boron concentration by banked movements of control rods. The methods of analysis described in Section 3 were used to calculate rodded and unrodded core constants and axial WANDA problems were run to obtain k_{eff}.

The fuel pellets were expanded with a UO_2 coefficient of expansion of $6.2 \times 10^{-6}/°F$. The stainless steel cladding was expanded with a SS-348 coefficient of $9.7 \times 10^{-6}/°F$ The H_2O volume was expanded with the same coefficient as stainless steel, since the water is contained in a stainless steel structure. A mass balance of all materials except water was maintained within the reactor boundaries. The atom densities of UO_2, stainless steel and Zr were obtained from the values at 68°F and 514°F by assuming a linear relationship with temperature. The H_2O atom densities were obtained from thermodynamic properties of compressed water [19]. A constant value of reflector savings was used in obtaining the geometric buckling. This should have a negligible effect on the calculations since leakage is small in a reactor of the size of Yankee. Before taking the derivative of the curve of k_{eff} against temperature, the calculated points were fitted to a polynomial by using the POLYFIT code.

Figure 6.1 shows the temperature coefficient as a function of boron concentration and temperature. The coefficient is negative and increases in absolute magnitude with temperature. The largest negative contribution to the coefficient is the change in U-238 resonance escape probability. At elevated temperatures, this change is a result mostly of the large change in moderation with temperature. Approximately 80% of the coefficient is a result of density changes, mostly H_2O, while the remaining 20% are spectrum and Doppler effects. This temperature coefficient should be properly called a zero power temperature coefficient, since the fuel was at the same temperature as the moderator in the calculations. One would expect a different rate of change in resonance escape probability with moderator temperature at higher fuel temperatures, but this should only amount to a few percent. A fourth degree polynomial fit was used to obtain the points of Figure 6.1. The slopes obtained from a parabola fit differed from these by approximately 10%. Since only two boron concentrations were considered at each temperature the second

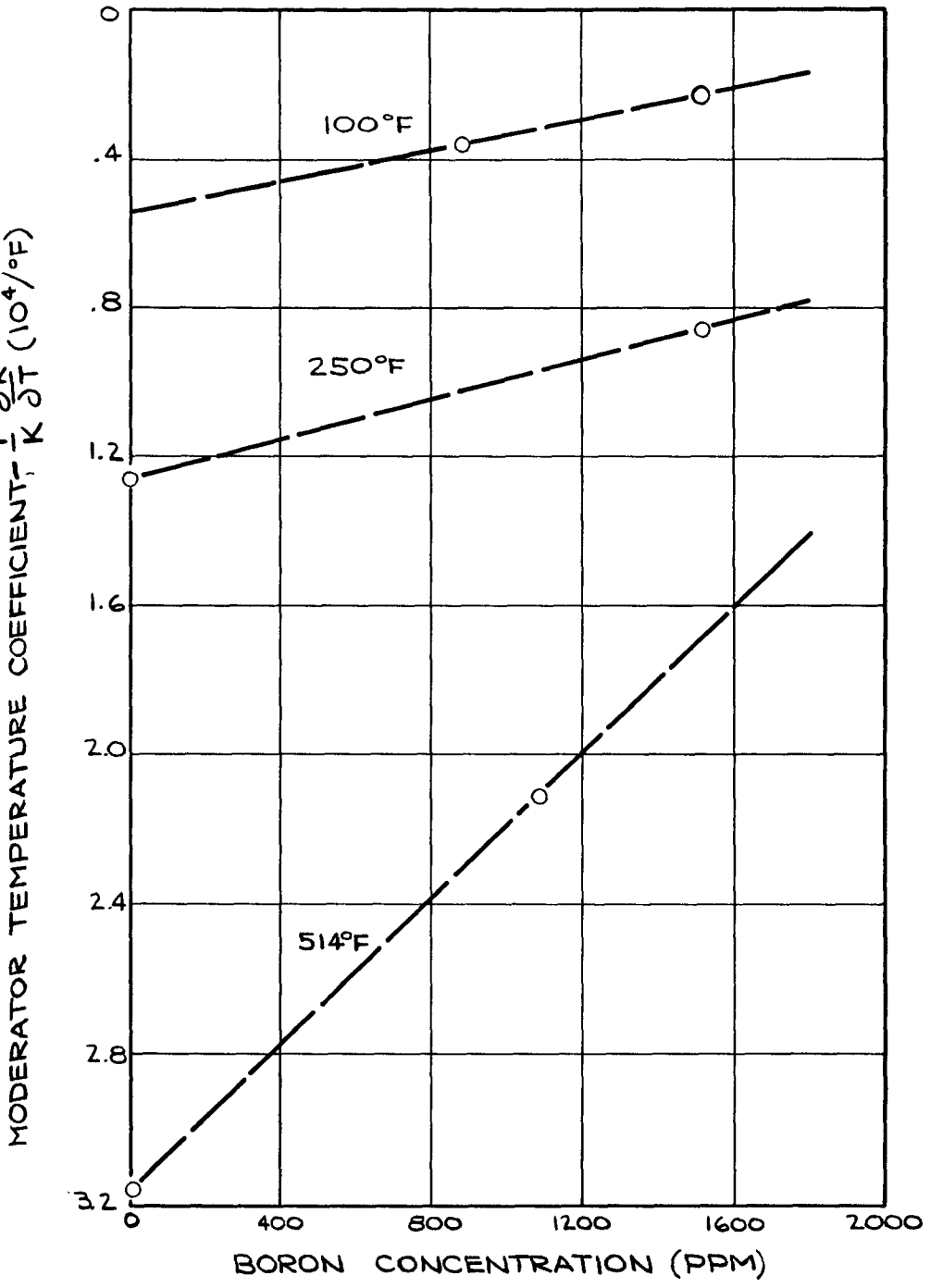

MODERATOR TEMPERATURE COEFFICIENT AS A FUNCTION OF BORON CONCENTRATION AND TEMPERATURE WITH BANKED RODS IN A CRITICAL CORE.

ED SK 288219C

Figure 6.1

derivatives of the curves in Figure 6.1 are not known and these are therefore arbitrary. Since the second derivatives are probably very small, straight lines were drawn for each temperature.

The values shown in Figure 6.1 are somewhat different from previous values given in former calculations of the Yankee kinetic characteristics [9,20]. The difference is mainly a result of the use of different methods of calculation*. One drawback of the method used in this report to calculate the temperature coefficient is the use of the MUFT fast constant code. The cross section library of the code, as it is now written, is temperature independent, and the code probably underestimates the resonance capture in U-235. It should be noted that these have only minor effects on the moderator temperature coefficient since the variation in water density with temperature is included in the MUFT calculations. As stated above, the water density variation is the most important effect and it determines in a very large part the variations in resonance absorption and the fast spectrum.

Since the temperature coefficient was calculated for a banked rod configuration, calculations were performed to study the effect of programmed rods on the temperature coefficient. This was done by running radial WANDA problems for various control rod configurations and comparing these with the axial WANDA problems for essentially critical configurations. To achieve this, the critical axial buckling was used in the calculations of the temperature coefficient for the programmed rod configurations. There was no difference between the temperature coefficients calculated for banked and programmed rod configurations. This study indicates that, for a uniform temperature distribution, the temperature coefficient is sensitive to the amount of reactivity being controlled by control rods, and relatively insensitive to the distribution of control rods required to achieve a given reactivity reduction.

---

* The moderator temperature coefficient in YAEC-73 was calculated on the basis of the four-factor formula. The calculation neglected epithermal fission in U-235 and resonance capture in coolant and structural materials. The largest difference is probably due to the different contributions of leakage since the calculations in YAEC-73 were done for a non-critical core.

The temperature coefficient is very sensitive to the type and amount of control in the core. The boron is a positive contribution to the coefficient while control rods are a negative contribution. The positive effect of boron is due to the decrease in thermal absorption with temperature, and the negative effect of control rods results from the decrease in core cross-section with temperature, which makes a black rod relatively more effective. If we define the effective multiplication factor as a product of an unrodded k and a control reduction factor R, the temperature coefficient may be written

$$\frac{1}{k_{eff}} \frac{\partial k_{eff}}{\partial T} = \frac{1}{k} \frac{\partial k}{\partial T} + \frac{1}{R} \frac{\partial R}{\partial T} . \qquad (6.2)$$

Figure 6.2 shows the contribution of the boron and of banked control rods to the temperature coefficient at operating temperature, together with the value of the temperature coefficient for a core without control. A neutron cycle model leading to a seven factor criticality formula [4] was used in the computation of the "no control" moderator temperature coefficient. The variation of each factor with moderator temperature was calculated, and the "no control" coefficient was obtained from the sum of the seven individual temperature coefficients.

Two methods were used in the calculation of the contribution of control rods to the moderator temperature coefficient. In the first method the contribution was obtained directly from the variation of the control rod reduction factor R with moderator temperature. In the second method, it was assumed that control rods influenced the moderator temperature coefficient only through thermal leakage and the thermal utilization. The contribution of control rods to the temperature coefficient was then obtained from a comparison of thermal leakage and thermal utilization coefficient for rodded and unrodded cores. The curve on Figure 6.2 represents an average of the results obtained from the two methods. Figure 6.2 can be conveniently used to obtain the temperature coefficient for various combinations of boron concentration and control rods. Because of the approximations made in obtaining these curves, Figure 6.2 is expected to compare to within 20% of the results of Figure 6.1.

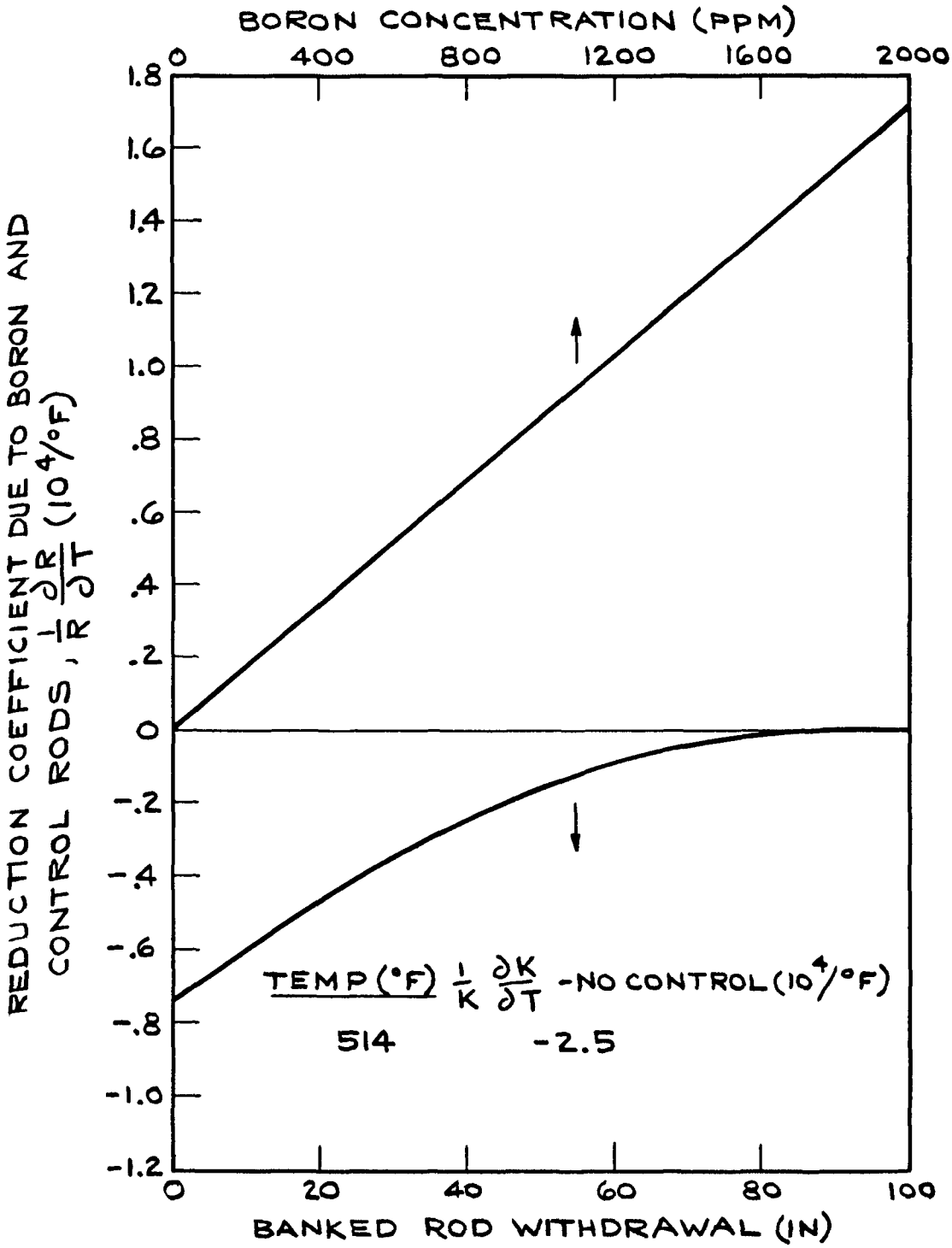

CONTRIBUTION OF BORON AND CONTROL RODS TO THE HOT MODERATOR TEMPERATURE COEFFICIENT

ED SK 288221C

Figure 6.2

The most important effect of reactor life on the moderator temperature coefficient arises from the removal of control rod to maintain criticality as depletion proceeds. As Figure 6.2 shows, the presence of fully inserted control rods adds a negative contribution of 0.74×10^{-4}/°F to the moderator coefficient. The effect of fission products, Pu buildup and fuel depletion on the unrodded temperature coefficient was obtained by using number densities from a study of fuel depletion performed with the use of the TURBO code [8] as input to SOFOCATE, since most of the change is expected to occur in the contribution of thermal utilization to the coefficient. The fission products Xe and Sm were represented explicitly and the other fission products were combined and assumed to have a 1/v cross section of 71 barns at 2200 m/sec. The changes in temperature coefficient are shown in Table 6.1 for the hot core.

Table 6.1

VARIATION OF THE UNRODDED ZERO BORON TEMPERATURE COEFFICIENT WITH REACTOR LIFE

Temperature °F	Life (Hrs.)	$\Delta \left(\frac{1}{k_{eff}} \frac{\partial k_{eff}}{\partial T}\right)$ 10^4/°F	Kg Pu / Kg U-235
514	100	+ 0.05	---
514	5,500	+ 0.20	0.093
514	10,000	+ 0.31	0.173

The table also gives values of kilograms of Pu/kilogram of U-235. At 100 hours, the change is due to the presence of Xe. The positive effect of Xe results from the rapid decrease of the Xe cross section with temperature. The further increase in temperature coefficient during lifetime is predominantly a result of U-235 depletion and Pu-239 buildup. The positive contribution of Pu-239 is a result of the resonance at 0.3 ev. The calculations used a value of α (capture to fission ratio) of 0.65 at the peak of the resonance. Recent measurements [25] would indicate a value which is 5 to 10% larger. This would make the positive Pu-239 contribution slightly less. Pu-240 is a negative contribution.

Thus, further increase in the Pu concentration would make the effect of Pu less positive. Such an effect was noticed in previous calculations [9].

The effects of fuel depletion and Pu buildup on the fast spectrum and the resonance capture contribution to the moderator temperature coefficient are not included in the values given in Table 6.1. Here again, these are minor effects compared to the effects of water density variation. The negative contribution of control rods at beginning of life is approximately $0.6 \times 10^{-4}/°F$. Using the values given in Table 6.1, as core life proceeds and the control rods are completely removed, the coefficient varies from $-3.2 \times 10^{-4}/°F$ to $-2.3 \times 10^{-4}/°F$.

6.2 Doppler and Power Coefficients

The Doppler coefficient of reactivity arises in heterogeneous reactors such as Yankee because of changes in temperature of the uranium oxide which results in a change in the thermal agitation of the uranium nuclei. Since a cross-section is a function of the relative energy of the neutron and the target nuclei, a change in temperature, which results in a change in the relative energy of neutron and nuclei, will affect the cross sections, especially fast varying cross-sections such as a resonance. The width, Γ, of a resonance increases with temperature and this results in a change in resonance escape probability, p. In a lumped fuel element, where the absorption is much larger than the scattering, the change in p is due mostly to the change in the width of the resonances.

The Doppler coefficient will be defined as the fractional change in multiplication factor per degree change in fuel temperature. We restrict our attention to the change in the U-238 resonance escape probability, p_{28}, and neglect the effect of U-235. The Doppler coefficient α_D is thus defined

$$\alpha_D = \frac{1}{p_{28}} \frac{\partial p_{28}}{\partial \bar{T}_f} \qquad (6.3)$$

where $\bar{T}_f$ is an effective fuel temperature. As mentioned above, the Doppler coefficient is a fast coefficient compared to the slower, although larger in magnitude, moderator temperature coefficient. In calculating the

Doppler coefficient it has been assumed that only the fuel temperature varied, while the moderator temperature stayed constant. If p_{28} is defined as

$$p_{28} = e^{-\frac{N_{28}}{\xi \Sigma_s} RI_{28}} \tag{6.4}$$

where RI_{28} is an effective resonance integral for U-238, the Doppler coefficient can be written

$$\alpha_D = \ell n\, p_{28}\, \frac{1}{RI_{28}}\, \frac{\partial RI_{28}}{\partial \overline{T}_f}. \tag{6.5}$$

The U-238 resonance integral temperature coefficient is a function of fuel temperature and rod size. The expression used in this report was

$$\frac{1}{RI_{28}}\, \frac{\partial RI_{28}}{\partial T_f} = \frac{\alpha}{2}\, \overline{T}_f^{-\frac{1}{2}} \tag{6.6}$$

where

$$\alpha = .00696 - .000262\ (S/M)^{-1} \tag{6.7}$$

and S/M is the surface to mass ratio of the uranium oxide. The expressions given in equations (6.6) and (6.7) are the result of a Monte Carlo study of the Doppler effect in UO_2 fuel [21]. This assumed a parabolic distribution of fuel temperature in the pellets. These expressions give results which are in good agreement with recent measurements by Hellstrand [22]. Figure 6.3 shows the variation of the U-238 resonance integral temperature coefficient with fuel temperature. The coefficient is positive, since the Doppler broadening of the U-238 resonances increases the effective resonance integral. The coefficient decreases with temperature since, once a resonance is broadened such that it overlaps neighboring resonances, further broadening will little effect the absorption. It should be noted that this does not explain the $T^{-1/2}$ law which seems to be a fortuitous result of conflicting trends.

Figure 6.4 shows the Doppler coefficient for two moderator temperatures, 60°F and 514°F. The Doppler coefficient is negative and

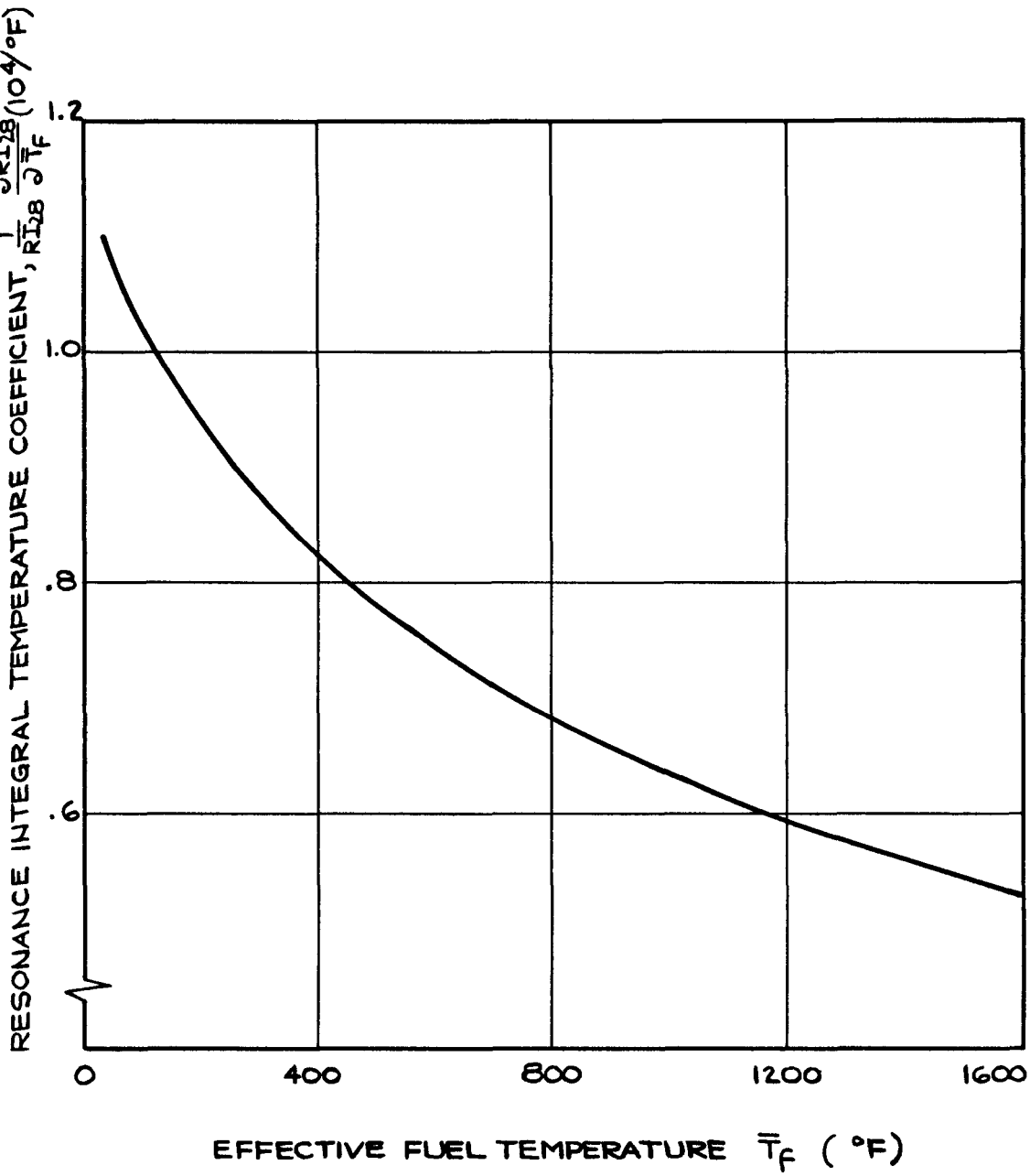

U-238 EFFECTIVE RESONANCE INTEGRAL TEMPERATURE COEFFICIENT VS. FUEL TEMPERATURE.

ED SK 2882200

Figure 6.3

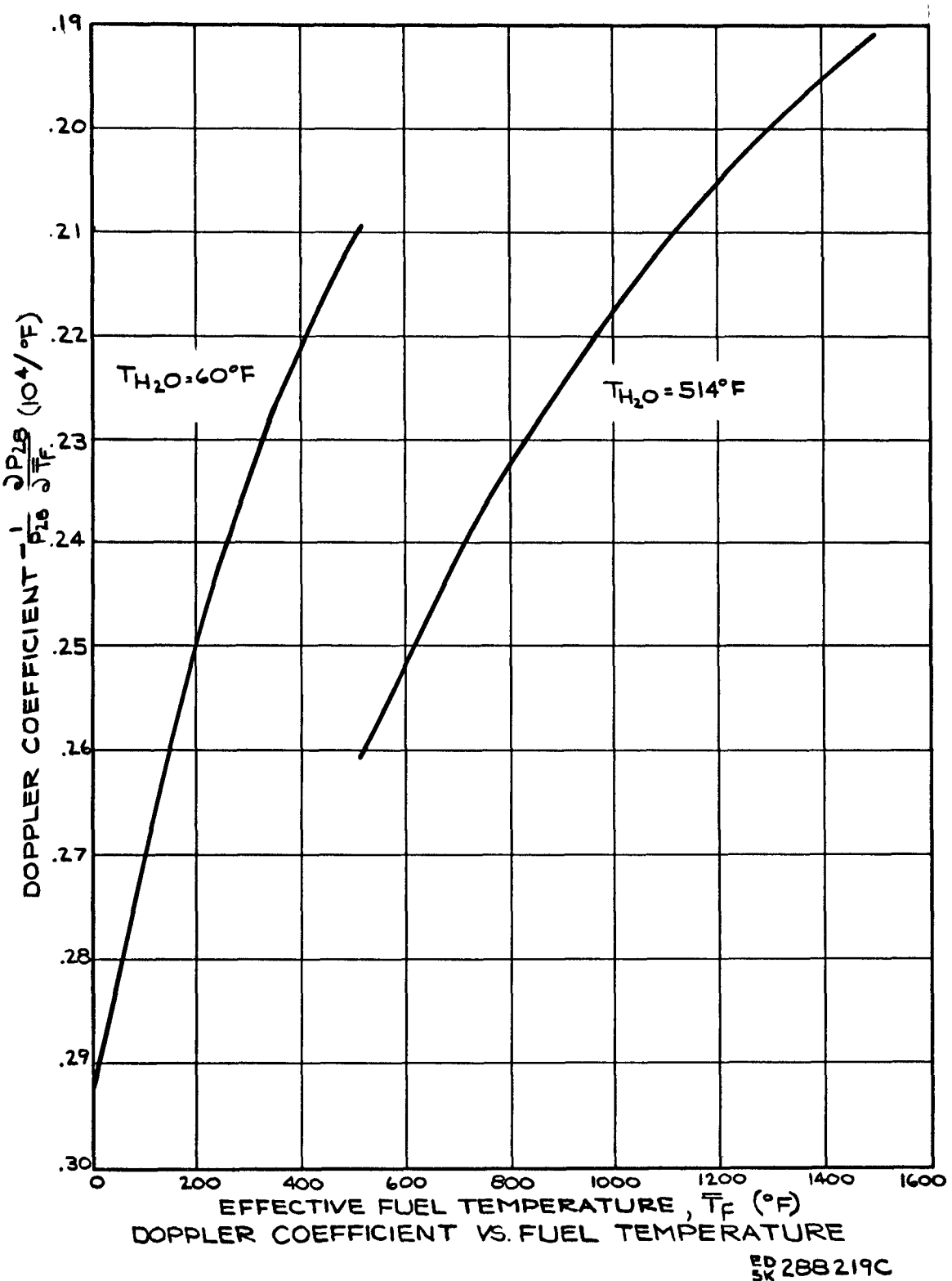
.19
.20
.21
.22
.23
.24
.25
.26
.27
.28
.29
.30
T_{H_2O}=60°F
T_{H_2O}=514°F
DOPPLER COEFFICIENT $-\frac{1}{P_{28}}\frac{\partial P_{28}}{\partial \bar{T}_F}$ (10^4/°F)
0
200
400
600
800
1000
1200
1400
1600
EFFECTIVE FUEL TEMPERATURE, $\bar{T}_F$ (°F)
DOPPLER COEFFICIENT VS. FUEL TEMPERATURE
ED SK 288219C

Figure 6.4

becomes less negative with temperature, since the resonance broadening becomes less important as the temperature is increased.

Since the fuel temperature is usually not a measurable quantity, what one actually measures in an experiment is a power coefficient. The power coefficient can be obtained from the Doppler coefficient at a constant moderator temperature of 514°F. This coefficient is a function of the effective fuel temperature. In obtaining a relation between effective fuel temperature and power, the following heat transfer coefficients were assumed. The temperature drop across the stainless steel clad and the coolant film was assumed constant at a value of 30°F. The drop in the gap between the fuel pellets and the stainless steel clad was obtained by assuming a constant heat transfer coefficient between zero and full power. The gap drop ΔT_g in °F as a function of percent full power is then given by

$$\Delta T_g = 4.46\ P \tag{6.8}$$

The variation in UO_2 thermal conductivity with fuel temperature was calculated from*

$$K_{UO_2} = \frac{3300}{\overline{T}_f + 460} \tag{6.9}$$

where $\overline{T}_f$ is in °F and K_{UO_2} has the unit of Btu/hr-ft-°F. The effective fuel temperature is given by

$$\overline{T}_f = T_s + .35\ (T_{max} - T_s) \tag{6.10}$$

where T_s is the fuel surface temperature and T_{max} is the temperature at the center of the fuel and $(T_{max} - T_s)$ is a function of power. The effective fuel temperature in °F as a function of percent full power is then given by the expression

$$\overline{T}_f = \frac{544 + 4.76\ P}{1 - .65 \times 10^{-3}\ P}\ . \tag{6.11}$$

---

* Personal communications - L. S. Tong, Westinghouse Electric Corporation, Atomic Power Department

The power coefficient is shown in Figure 6.5 as a function of power. Although the power coefficient varies by only 5% from zero to full power, the Doppler effect will depend strongly on the power shape in the core. The curve of Figure 6.5 assumes a uniform power distribution. A statistical weight factor which depends on the power shape should therefore be applied to the power coefficient. Radial WANDA problems were run for various control rod configurations using equation (5.1) of Section 5.6 with the appropriate values of P_R/P_{Avg} to represent the Doppler effect in each radial region, R. In some of the problems the radial distribution in coolant temperature was taken into account by the expression

$$T_{H_2O_R} = 499 + (33/2)\, P_R/P_{Avg} \ ^\circ F. \qquad (6.12)$$

Statistical weight factors were obtained by comparing the Doppler effect for uniform and non-uniform power distributions. Table 6.2 gives the statistical weight factors for the power coefficient for four control rod configurations. An axial weight factor of 1.26 was applied in all cases. This factor (K_{axial}) was computed from perturbation theory. The fast flux was taken to be self-adjoint and a constant fast to thermal flux ratio was assumed in the axial direction. The axial variation in power was assumed to be a chopped cosine in all cases. K_{axial} is thus given by

$$K_{axial} = \frac{\overline{\varphi^3}}{\overline{\varphi}\ \overline{\varphi^2}} \qquad (6.13)$$

Table 6.2

STATISTICAL WEIGHT FACTORS FOR THE POWER COEFFICIENTS

Rod Array	K_D	$K_{D,T}$
0	1.79	1.95
1	1.48	1.54
135	1.31	1.27
12345	1.32	1.39

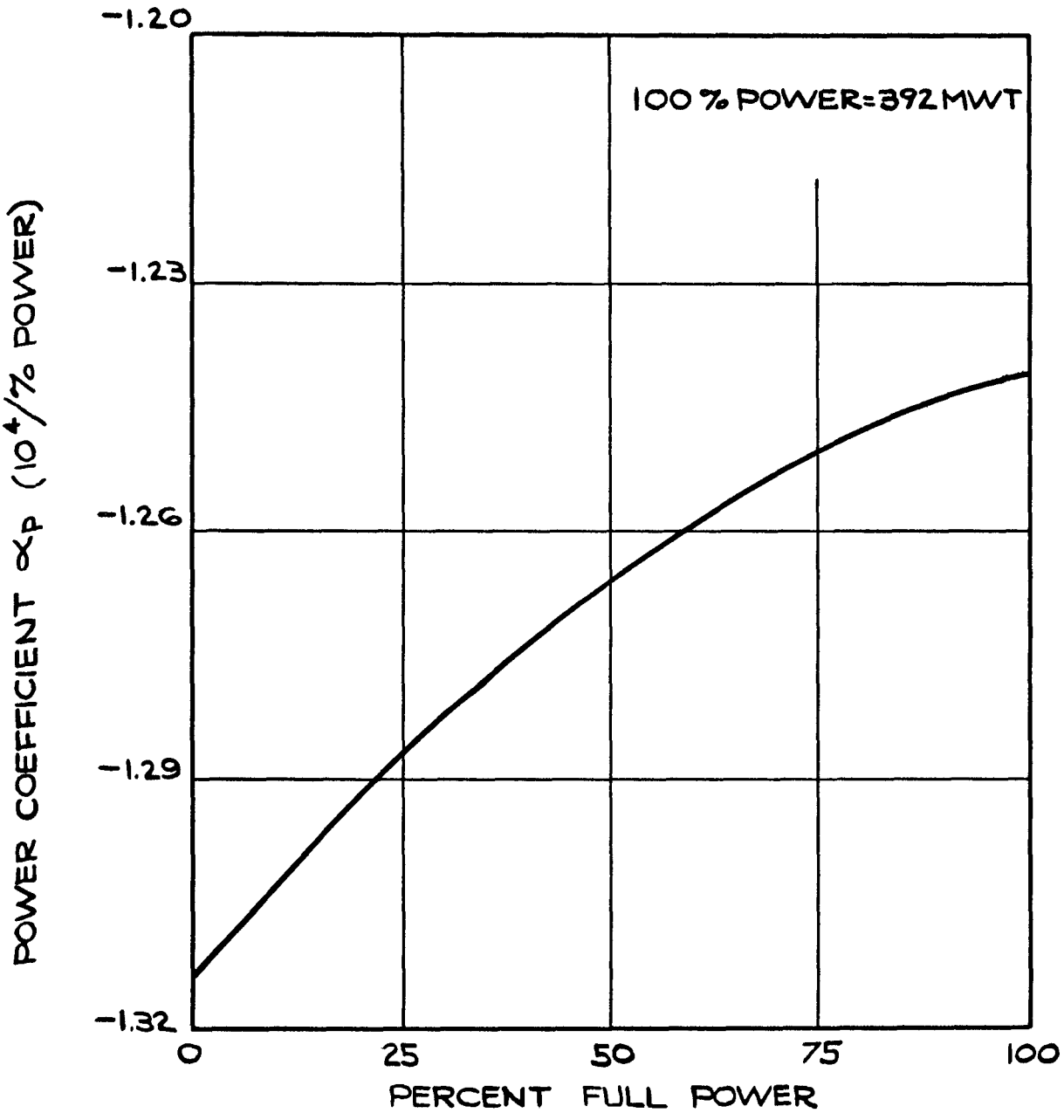

POWER COEFFICIENT VS. POWER LEVEL AT A MODERATOR TEMPERATURE OF 514° F

Figure 6.5

ED SK 288220C

In Table 6.2, K_D takes into account the power shape while $K_{D,T}$ takes into account both the power shape and coolant temperature distribution. The values given in Table 6.2 indicate that the negative power coefficient will increase as core life proceeds and control rods are removed. The effect will not be as great as indicated since the non-uniform fuel depletion will tend to flatten the power in the core and reduce the values of the statistical weights. The statistical weight factors for Xe and Sm given in Section 5.6 were obtained by a similar method and the use of equations (5.2) and (5.3). In this case the axial factors were 1.06 for Xe and Sm, and 1.09 for Doppler and Xe and Sm combined.

6.3 Pressure and Void Coefficients

The pressure coefficient was obtained from the temperature coefficient by separating the density from the spectrum and fuel effects, thus obtaining a rate of change in k_{eff} with H_2O atom density. The density contribution of other core materials was neglected. The variation of H_2O atom density with pressure at a constant temberature was then obtained from reference [19] and the pressure coefficient calculated.

A void coefficient was calculated by assuming that a change in H_2O atom density corresponded to a change in percent void present in the core. This coefficient assumes a uniform distribution of voids in the reactor. Table 6.3 shows the pressure and void coefficients at 514°F and two boron concentrations.

Table 6.3

PRESSURE AND VOID COEFFICIENTS

Temperature °F	Boron Conc. (ppm)	Pressure (psig)	$\frac{1}{k_{eff}} \frac{\partial k_{eff}}{\partial P}$ (10^6/psig)	$\% \frac{\partial k}{k} / \%$ Void
514	0	2000	+ 2.5	-.22
514	1080	2000	+ 1.4	-.12

The pressure coefficient is positive and therefore opposes the temperature coefficient since an increase in temperature tends to cause a corresponding increase in pressure. In general, this will only slightly decrease the effect of the temperature coefficient because of the presence in the coolant loop of a pressurizer which tends to maintain a constant system pressure and because the pressure coefficient is much smaller in magnitude*.

It should be noted, as regards the void coefficient, that no voids are expected at any time in Yankee. If voids were present, a statistical weight factor should be applied to the void coefficient since the effect of voids depend on their locations in the core. For a large reactor such as Yankee, the leakage effect is small and the effect of voids will be mostly a change in k_∞ resulting from a change in p_{28} due to the decrease in moderation caused by the voids. One should also take into account the fact that the production of voids depends also on the power shape. As a rough approximation, the statistical weight factor applied to the power coefficient in Table 6.2 can be applied to the void coefficient.

The effect of fission product buildup, Pu buildup, and fuel depletion on the pressure and void coefficients has been shown to be less than 10% during the lifetime of the reactor [9,20].

6.4 Prompt Neutron Lifetime

The prompt neutron lifetime ℓ^* was calculated by the following two-group expression [23]:

$$\ell^* = \frac{D_f/\tau}{v_f}\left(\frac{1}{1+\tau B^2}\right) + \frac{\Sigma_a}{v_s}\left(\frac{\nu_{28}-1}{\nu_{28}\epsilon - 1}\right)\frac{1}{\beta}\left(\frac{1}{1+L^2B^2}\right) \qquad (6.14)$$

where the subscripts f and s refer to the fast and thermal groups, v is the neutron velicity, ν_{28} is the number of neutrons emitted per fast fission in U-238, ϵ is the fast fission factor and β is the multiplication

---

* This is true of most practical cases; however, if the pressurizer steam "bubble" is collapsed, the pressure coefficient would override the temperature coefficient. This occurrence is guarded against by proper sizing of the pressurizer and thus does not present a plant hazard.

factor for epithermal fission in U-235. The values of neutron velocity were obtained from outputs of MUFT and SOFOCATE, and unrodded core constants were used in equation (6.14). Criticality was maintained by using a critical buckling for B^2. This in effect assumes that the banked movement of control rods corresponds to a change in water height for the core. Table 6.4 gives the prompt neutron lifetime at 514°F and two boron concentrations.

Table 6.4

PROMPT NEUTRON LIFETIME

Temperature °F	Boron Conc. (ppm)	ℓ^* (10^4 sec^{-1})
514	0	.20
514	1080	.18

6.5 Effective Delayed Neutron Fraction

The effective delayed neutron fraction, β_{eff}, differs from the delayed neutron fraction for U-235 because the fast fission in U-238, with its greater delayed neutron yield, tends to increase the delayed neutron fraction for the core, and because delayed neutrons are born with an energy spectrum significantly different from that of the prompt neutrons. This in effect gives delayed neutrons a different importance or effectiveness in contributing to the neutron cycle. It is convenient to define β_{eff} as the product of an average delayed neutron fraction $\bar{\beta}$, averaged according to the fission rates and delayed neutron yields of U-235 and U-238, and a delayed neutron importance function $\bar{I}$. The derivation of the Inhour formula by the perturbation method [26] leads to a definition of β_{eff} as the ratio of fission neutrons produced by capture of the delayed neutrons to the total number of fission neutrons produced by cycle. Since β_{eff} was defined as the product of the average delayed neutron fraction $\bar{\beta}$ and the importance function $\bar{I}$, this importance function is then defined as the ratio of fission neutrons produced with a source of one delayed neutron to the number of fission neutrons produced with a source of one prompt neutron. The SOFOCATE thermal constant code and the MUFT fast constant

code were used with both prompt and delayed neutron source spectra to calculate $\bar{I}$. A ratio of U-238 fissions to U-235 fissions of 0.09 was used in the calculation of $\bar{\beta}$. The delayed neutron data was that of Keepin[27]. These calculations yielded a value of $\bar{\beta}$ of 0.00720 and a value of $\bar{I}$ of 1.0121, or a value of 0.00729 for β_{eff}, for the hot, clean core at beginning of life.

6.6 Xenon and Samarium Transient Effects

Figure 6.6 shows the buildup of Xe-135 after shutdown at the beginning of core life. The curve was calculated with the use of xenon tables [24] and assumed equilibrium xenon at shutdown. The peak occurs at about 6 hours after shutdown and the maximum negative reactivity introduced by xenon is approximately 2.6%. In using this curve, it should be noted that Sm-149 has not been considered. At equilibrium, the samarium poisoning in Yankee is about one-third that of xenon. For a thermal flux of the order of that encountered in Yankee, the equilibrium promethium concentration, in terms of samarium atoms, is about one-fourth that of samarium. Then after a shutdown, Sm will build up to approximately 125% of its equilibrium value, but the half life associated with this buildup is longer than that for xenon. Based on these estimates, the maximum Sm poisoning after shutdown is approximately 1%. It should also be noted that since Sm-149 is a stable isotope, the negative reactivity introduced by Sm constitutes a permanent reduction in k_{eff}.

Since Figure 6.6 assumes a uniform power distribution in the core, statistical weight factors should be applied to it. This statistical factor is of the order of the statistical factor applied to the equilibrium Xe and Sm, but it will be time dependent, since the xenon poisoning is time dependent.

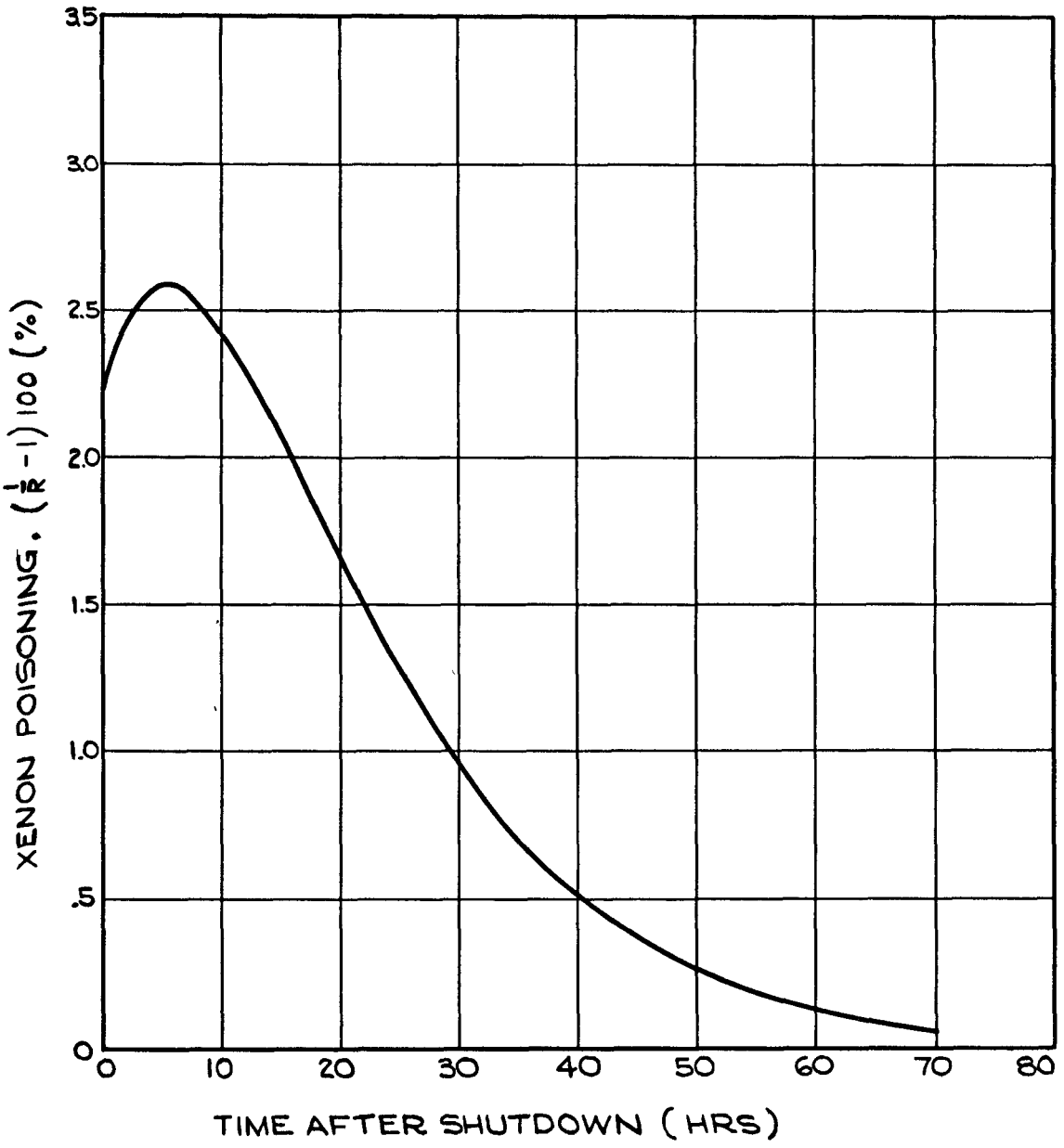

Xe^{135} TRANSIENT AFTER SHUTDOWN

Figure 6.6

E.D. SK. 288215-C

7.0 SUMMARY OF NUCLEAR DATA

(Beginning of Core Life)

Reactivity Characteristics	
k_{eff} (cold, clean)	1.167
k_{eff} (hot, clean, zero power)	1.113
k_{eff} (hot, clean, full power*)	1.089
k_{eff} (hot, equilibrium poison, full power)	1.060
Control Characteristics (24 Control Rods)	
Rod Worth (68°F, zero boron) **	14.8
(68°F, 1200 ppm boron)	13.8
(514°F, zero boron)	18.2
Boron Worth (cold, zero boron)	0.8×10^{-4}/ppm
(hot, zero boron)	0.7×10^{-4}/ppm
Kinetic Characteristics	
Moderator Coefficient (cold, 1200 ppm boron)	$-3. \times 10^{-5}$/°F
(hot, 1200 ppm boron)	$-2. \times 10^{-4}$/°F
(hot, zero boron)	$-3. \times 10^{-4}$/°F
Power Coefficient (zero power)	-1.3×10^{-4}/% power
(full power)*	-1.2×10^{-4}/% power
Pressure Coefficient (hot, zero boron)	$+2.6 \times 10^{-6}$/psig
Void Coefficient (hot, zero boron)	-2.2×10^{-3}/% void
Delayed Neutron Fraction	0.007
Prompt Neutron Lifetime	0.2×10^{-4} sec.

---

* 392 Mw Thermal

** $(1/R - 1)$; $R = k_{\text{with rods}}/k_{\text{without rods}}$

BIBLIOGRAPHY

1. P. W. Davison, et. al., "Yankee Critical Experiments Measurements on Lattices of Stainless Steel Clad Slightly Enriched Uranium Dioxide Fuel Rods in Light Water," YAEC-94 (1959).

2. P. W. Davison, et. al., "Two-Region Critical Experiments with Water Moderated Slightly Enriched UO_2 Lattice," YAEC-142 (1959).

3. R. A. Dannels, W. J. Eich, "Neutron Flux Peaking and Power Shapes: A Comparison of Theory and Experiment," YAEC-151 (1959).

4. W. H. Arnold, Jr., "Critical Masses and Lattice Parameters of H_2O-UO_2 Critical Experiments: A Comparison of Theory and Experiment," YAEC-152, (1959).

5. E. A. McCabe, Jr., "Thermal Design Aspects of the Yankee First Core Fuel Rod," YAEC-106 (1960).

6. H. W. Graves, Jr., et. al., "A Study of Loading Configurations for the Yankee Reactor," YAEC-114 (1959).

7. M. Robkin, "Yankee Control Rod Programming Study," YAEC-164 (1959).

8. J. D. McGaugh, "A Study of Fuel Depletion and Control Rod Programming in the Yankee Reactor," YAEC-183 (1961).

9. "Yankee Atomic Electric Company, Technical Information and Final Hazards Summary Report," Part B, License Application, AEC Docket No. 50-59, Vol. 1 (1959).

10. R. R. McCready, D. B. Vollenweider, "An IBM-704 Program for the Solution of the Neutron Transport Equation in Fifty Concentric Cylindrical Annuli by the Weil Method, Program I_2," APEX-468.

11. H. Amster, R. Suarez, "The Calculation of Thermal Constants Averaged Over a Wigner Wilkins Flux Spectrum: Description of the SOFOCATE Code, WAPD-TM-39 (1957).

12. C. P. Wigner, J. E. Wilkins, Jr., "Effect of the Temperature of the Moderator on the Velocity Distribution of Neutron with Numerical Calculations for H as Moderator," AECD-2275 (1944).

13. H. Bohl, Jr., E. M. Gelbard, G. H. Ryan, "MUFT-4 Fast Neutron Spectrum Code for the IBM-704," WAPD-TM-72 (1957).

14. A. G. Thorp II, "Design of the Yankee Core I Fuel Assembly," YAEC-154 (1960).

15. O. J. Marlowe, C. P. Saalbach, L. M. Culpepper, D. S. McCarty, "WANDA - A One-Dimensional Few Group Diffusion Equation Code for the IBM-704," WAPD-TM-28 (1956).

16. G. G. Bilodeau, W. R. Cadwell, J. P. Dorsey, J. G. Fairey, R. S. Varga, "PDQ - An IBM-704 Code to Solve the Two-Dimensional Few Group Neutron Diffusion Equation," WAPD-TM-70 (1957).

17. W. H. Arnold, Jr., "Physics Calculations for Control Rods in the First Yankee Core," YAEC-62 (1959).

18. Review of Methods Used in Control Rod Analysis for Reactor Design at Bettis Plant - BT4 1 Number 4, pages 1-6.

19. T. C. Tsu and D. T. Beecher, "Thermodynamic Properties of Compressed Water," Westinghouse Research Laboratories.

20. W. H. Arnold, Jr., H. C. Hecker, Jr., "Moderator Temperature Coefficient of the Yankee Reactor as Presented in the Yankee Preliminary Hazards Summary Report," YAEC-73 (1958).

21. W. H. Arnold, Jr., and R. A. Dannels, "The Doppler Coefficient of U-238 O_2," Transactions of the American Nuclear Society 3-1, (1960).

22. E. Hellstrand , et. al., "The Temperature Coefficient of the Resonance Integral for Uranium Metal and Oxide," Nuclear Science and Engineering: 8, 497-506 (1960).

23. W. H. Arnold, Jr., "Two-Group Calculation on Prompt Neutron Lifetime," Nuclear Science and Engineering 4, 508 (1958).

24. H. K. Clark and J. C. English "Xenon Tables," DP-200 (1957).

25. "Neutron Cross Sections," BNL-325, Supplement No. 1 (1960).

26. A. F. Henry, "Computation of Parameters Appearing in the Reactor Kinetics Equations," WAPD-142 (1955).

27. G. R. Keepin, et. al., "Delayed Neutrons from Fissionable Isotopes of Uranium, Plutonium, Thorium," Phys. Rev. 107, 1044-1049, (1957).

28. A. D. Voorhis, et. al., "Experimental and Theoretical Study of Critical Slabs - Effect of Absorbing Membranes of Cadmium, Gold, and Boron," WAPD-170 (1957).

29. R. J. French, "The Dancoff Correction to the Resonance Absorption in Close-Packed Cylindrical Fuel Rod Lattices," YAEC-149 (1960).

ACKNOWLEDGEMENTS

The nuclear design calculations described in this report are the result of the effort of a large number of people. The authors would particularly like to acknowledge Messrs. J. D. McGaugh, H. T. Williams, and R. J. Nodvik for their assistance in performing these calculations. Core material specifications were provided by D. G. Brunstetter from the Quality Control and Inspection Group. The typing of the report, from the first draft to the final form, was very ably performed by Mrs. Mary Jane Kelly.

APPENDIX A

THERMAL CONSTANTS IN DISCRETE SLOT WATER AND ZIRCONIUM REGIONS

Slot Water

By definition,

$$\Sigma_{tr} = \frac{1}{3\,D} = \Sigma_a + \Sigma_s\,(1 - \bar{\mu}), \text{ where}$$

Σ_{tr} = thermal transport cross section (cm^{-1})

Σ_a = thermal absorption cross section (cm^{-1})

Σ_s = thermal scattering cross section (cm^{-1})

D = thermal diffusion coefficient (cm).

The thermal constants (D, Σ_a) for the "fuel" region, defined in Section 3.1, were obtained directly from SOFOCATE problems. It follows that,

$$\left(\frac{1}{3\,D} - \Sigma_a\right) = \Sigma_s\,(1 - \bar{\mu}) = \sum_i N_i \left[\sigma_s\,(1 - \bar{\mu})\right]_i + N_{H_2O}\left[\sigma_s\,(1 - \bar{\mu})\right]_{H_2O}$$

where $\sum_i N_i \left[\sigma_s\,(1 - \bar{\mu})\right]_i$ = sum of scattering contributions of all elements in the "fuel", except water, to the "fuel" thermal transport cross section.

Then,

$$(\Sigma_{tr})_{H_2O} = N_{H_2O}\,(2\,\sigma_{a,H} + \sigma_{a,O}) + \left(\frac{1}{3\,D} - \Sigma_a\right) - \sum_i N_i \left[\sigma_s\,(1 - \bar{\mu})\right]_i .$$

Accounting for the B-10 in the water slot,

$$(\Sigma_a)_{H_2O + B\text{-}10} = N_{H_2O}\,(2\,\sigma_{a,H} + \sigma_{a,O}) + N_{B\text{-}10}\,(\sigma_{a,B\text{-}10})$$

and

$$(D)_{H_2O + B\text{-}10} = \frac{1}{3\left\{(\Sigma_{tr})_{H_2O} + N_{B\text{-}10}\left[\sigma_a + \sigma_s\,(1 - \bar{\mu})\right]_{B\text{-}10}\right\}}$$

All microscopic absorption cross sections were obtained from the SOFOCATE output while values of $\left[\sigma_s\ (1 - \bar{\mu})\right]_i$ were obtained from the SOFOCATE cross section library.

Zirconium

$$\Sigma_a = N_{Zr}\ \sigma_{a,Zr}$$

$$D = \frac{1}{3\left\{ N \left[\sigma_a + \sigma_s\ (1 - \bar{\mu})\right]_{Zr}\right\}}$$

The microscopic cross sections were obtained from SOFOCATE as above.

The simplified expression used for zirconium may be used because the quantity $\sigma_s\ (1 - \bar{\mu})$ is independent of energy within the thermal energy group. However, the scattering cross section for hydrogen in the slot water does vary with energy and a spectrum averaged cross section must therefore be used.

APPENDIX B

EQUIVALENT ABSORPTION CROSS SECTIONS OF DOPPLER AND FISSION PRODUCT POISONING EFFECTS

Doppler

The power coefficient is defined as follows:

$$\alpha_p = \frac{1}{k_{eff}} \frac{\Delta k_{eff}}{\Delta p}$$

or

$$\alpha_p \Delta p = \frac{\Delta k_{eff}}{k_{eff}}.$$

At zero power,

$$k_{eff} = \frac{\nu\Sigma_{ff}}{A_1} + \frac{\nu\Sigma_{ff}\,\Sigma_r}{A_1\,A_2},$$

where

$$A_1 = D_f B^2 + \Sigma_{af} + \Sigma_r$$

$$A_3 = D_s B^2 + \Sigma_{as}.$$

At power,

$$k^1_{eff} = \frac{\nu\Sigma_{ff}}{A_1 + \Delta\Sigma_{af}} + \frac{\nu\Sigma_{ff}\,\Sigma_r}{(A_1 + \Delta\Sigma_{af})\,A_2},$$

where $\Delta\Sigma_{af}$ = contribution of Doppler broadening of the capture resonances in U-238 to the fast absorption cross section in the core. Subtracting

$$\Delta k_{eff} = k^1_{eff} - k_{eff} = k_{eff}\left(-\frac{\Delta\Sigma_{af}}{A_1 + \Delta\Sigma_{af}}\right),$$

$$\frac{\Delta k}{k} = \alpha_p \Delta p = \frac{\Delta\Sigma_{af}}{A_1 + \Delta\Sigma_{af}},$$

solving for $\Delta\Sigma_{af}$,

$$\Delta\Sigma_{af} = \left(- \frac{\alpha_p \Delta p}{\alpha_p \Delta p + 1} \right) A_1 .$$

In a multiregion core the power generated in each region is simply

$$\Delta p_R = \left(\frac{P_R}{P_{average}} \right) \Delta p ,$$

where

P_R = average power in region R

$P_{average}$ = average power in the core.

A regionwise power coefficient may then be defined as,

$$(\alpha_p)_R = \alpha_p \left(\frac{P_R}{P_{average}} \right) .$$

Therefore, $\Delta\Sigma_{af}$ per region is given by,

$$\Delta\Sigma_{af,R} = \frac{-\Delta p \ \alpha_p \ (P_R/P_{avg})}{\Delta p \ \alpha_p \ (P_R/P_{avg}) + 1} \quad (\Sigma_{af} + \Sigma_r + D_f B^2)$$

Xenon

The equilibrium concentration of Xe is given by:

$$N_{Xe} = \frac{Y_{Xe} \ (\varphi_1 \Sigma_{f1} + \varphi_2 \Sigma_{f2})_{avg}}{\lambda_{Xe} + \sigma_{Xe} \ \varphi_{2,avg}} \quad /14$$

or

$$\Sigma_{a,Xe} = \frac{Y_{Xe} \ (\varphi_1 \Sigma_{f1} + \varphi_2 \Sigma_{f2})_{avg}}{\frac{\lambda_{Xe}}{\sigma_{Xe}} + \varphi_{2,avg}} .$$

Y_{Xe} = yield per fission of Xe.

λ_{Xe} = decay constant for Xe

σ_{Xe} = Xe thermal absorption cross section.

The subscripts "1" and "2" refer to fast and thermal energy groups. The regionwise cross section is therefore:

$$\Sigma_{a,Xe,R} = \frac{Y_{Xe}\,(\varphi_1\,\Sigma_{f1} + \varphi_2\,\Sigma_{f2})(P_R/P_{avg})}{\frac{\lambda_{Xe}}{\sigma_{Xe}} + \varphi_{2,avg}\,(P_R/P_{avg})} \quad .$$

Samarium

Assuming a uniform distribution of Sm in the core, the absorption cross section is given by,

$$\Sigma_{a,Sm} = N_{Sm}\,\sigma_{Sm} = \frac{Y_{Sm}\,(\varphi_1\,\Sigma_{f1} + \varphi_2\,\Sigma_{f2})}{\varphi_{2\ avg}} \quad ,$$

where N_{Sm} is the equilibrium concentration of Sm /14.

APPENDIX C

NUCLEAR CONSTANTS OF CORE AND REFLECTOR AT 100°F

Table C-1

HOMOGENIZED RODDED CORE CONSTANTS AT 100°F

	Thermal			Fast			
C_B (ppm)	Σ_a	$\nu\Sigma_f$	D	D	Σ_a	Σ_r	$\nu\Sigma_f$
0	.15451	.21535	.27680	1.13920	.014897	.019264	.0096437
430	.15925	.21352	.27737	1.13935	.015000	.019180	.0096370
590	.16100	.21283	.27758	1.13940	.015039	.019144	.0096343
650	.16160	.21260	.27765	1.13942	.015053	.019137	.0096335
860	.16393	.21172	.27793	1.13949	.015104	.019096	.0096301
1510	.17106	.20888	.27871	1.13971	.015259	.018969	.0096198
1940	.17573	.20707	.27919	1.13985	.015362	.018884	.0096130
2160	.17806	.20619	.27941	1.13993	.015414	.018843	.0096096

Table C-2

HOMOGENIZED UNRODDED CORE CONSTANTS AT 100°F

	Thermal			Fast			
C_B (ppm)	Σ_a	$\nu\Sigma_f$	D	D	Σ_a	Σ_r	$\nu\Sigma_f$
0	.13642	.20437	.30247	1.14638	.012665	.019222	.0094164
430	.14105	.20270	.30292	1.14652	.012766	.019140	.0094105
590	.14280	.20207	.30308	1.14657	.012804	.019108	.0094083
650	.14336	.20185	.30315	1.14659	.012817	.019098	.0094075
860	.14569	.20103	.30335	1.14666	.012867	.019056	.0094046
1510	.15266	.19846	.30397	1.14687	.013019	.018931	.0093957
1940	.15723	.19682	.30436	1.14702	.013120	.018849	.0093897
2160	.15951	.19601	.30453	1.14709	.013171	.018809	.0093867

Table C-3

HOMOGENIZED RODDED REFLECTOR CONSTANTS AT 100°F

	Thermal			Fast			
C_B (ppm)	Σ_a	$\nu\Sigma_f$	D	D	Σ_f	Σ_r	$\nu\Sigma_f$
0	.059055	0	.18382	1.20686	.0045170	.039578	0
430	.069265	0	.18560	1.20710	.0047130	.039405	0
590	.073120	0	.18627	1.20719	.0047860	.039339	0
650	.074460	0	.18649	1.20722	.0048110	.039318	0
860	.079373	0	.18731	1.20734	.0049091	.039231	0
1510	.095130	0	.19012	1.20770	.0052072	.038968	0
1940	.105212	0	.19184	1.20794	.0054044	.038795	0
2160	.110268	0	.19265	1.20806	.0055025	.038709	0

Table C-4

HOMOGENIZED UNRODDED REFLECTOR CONSTANTS AT 100°F

	Thermal			Fast			
C_B (ppm)	Σ_a	$\nu\Sigma_f$	D	D	Σ_a	Σ_r	$\nu\Sigma_f$
0	.053180	0	.18382	1.20686	.002061	.039578	0
430	.063100	0	.18560	1.20710	.002256	.039405	0
590	.066850	0	.18627	1.20719	.002330	.039339	0
650	.068150	0	.18649	1.20722	.002355	.039318	0
860	.072937	0	.18731	1.20734	.002453	.039231	0
1510	.088228	0	.19012	1.20770	.002751	.038968	0
1940	.098040	0	.19184	1.20794	.002948	.038795	0
2160	.102965	0	.19265	1.20806	.003046	.038709	0

Table C-5

REGIONWISE CONSTANTS AT 100°F

Region	C_B (ppm)	Thermal			Fast			
		Σ_a	$\nu\Sigma_f$	D	D	Σ_a	Σ_r	$\nu\Sigma_f$
Fuel	0	.14476	.21838	.27756	1.14077	.013306	.019310	.009906
	860	.15424	.21438	.27881	1.14107	.013513	.019136	.009894
	1510	.16121	.21155	.27962	1.14130	.013666	.019006	.009884
	2160	.16807	.20886	.28033	1.14152	.013818	.018878	.009874
Water Slot	0	.013978	---	.21640	1.20768	.00057255	.044864	---
	860	.036195	---	.21713	1.20791	.0010030	.044777	---
	1510	.052394	---	.21756	1.20811	.0013249	.044712	---
	2160	.068228	---	.21791	1.20828	.0016458	.044648	---
Zirconium	0	.0049040	---	.95700	1.28327	.00010649	.00021713	---
	860	.0048222	---	.95725	1.28337	.00010629	.00021671	---
	1510	.0047639	---	.95736	1.28344	.00010613	.00021640	---
	2160	.0047085	---	.95755	1.28351	.00010598	.00021609	---

APPENDIX D

NUCLEAR CONSTANTS OF CORE AND REFLECTOR AT 514°F

Table D-1

HOMOGENIZED RODDED CORE CONSTANTS AT 514°F

	Thermal			Fast			
C_B (ppm)	Σ_a	$\nu\Sigma_f$	D	D	Σ_a	Σ_r	$\nu\Sigma_f$
0	.12524	.17458	.35934	1.26470	.014687	.014108	.0092012
270	.12736	.17398	.35930	1.26482	.014740	.014065	.0091971
540	.12948	.17338	.35925	1.26493	.014791	.014024	.0091931
810	.13158	.17280	.35920	1.26503	.014841	.013984	.0091890
1080	.13369	.17222	.35914	1.26512	.014889	.013947	.0091850

Table D-2

HOMOGENIZED UNRODDED CORE CONSTANTS AT 514°F

	Thermal			Fast			
C_B (ppm)	Σ_a	$\nu\Sigma_f$	D	D	Σ_a	Σ_r	$\nu\Sigma_f$
0	.10990	.16632	.38152	1.27205	.012244	.014107	.0090139
270	.11198	.16577	.38147	1.27217	.012296	.014066	.0090102
540	.11403	.16523	.38140	1.27228	.012347	.014026	.0090065
810	.11608	.16470	.38133	1.27238	.012396	.013987	.0090028
1080	.11812	.16418	.38124	1.27247	.012442	.013950	.0089992

Table D-3

HOMOGENIZED RODDED REFLECTOR CONSTANTS AT 514°F

	Thermal			Fast			
C_B (ppm)	Σ_a	$\nu\Sigma_f$	D	D	Σ_a	Σ_r	$\nu\Sigma_f$
0	.04417	0	.27082	1.43888	.004347	.030957	0
270	.04840	0	.27136	1.43907	.004444	.030871	0
540	.05265	0	.27185	1.43925	.004543	.030784	0
810	.05680	0	.27232	1.43944	.004640	.030698	0
1080	.06096	0	.27278	1.43962	.004737	.030613	0

Table D-4

HOMOGENIZED UNRODDED REFLECTOR CONSTANTS AT 514°F

	Thermal			Fast			
C_B (ppm)	Σ_a	$\nu\Sigma_f$	D	D	Σ_a	Σ_r	$\nu\Sigma_f$
0	.037319	0	.27082	1.43888	.001892	.030957	0
270	.041540	0	.27136	1.43907	.001990	.030871	0
540	.045796	0	.27185	1.43925	.002088	.030784	0
810	.049950	0	.27232	1.43944	.002185	.030698	0
1080	.054108	0	.27278	1.43962	.002282	.030613	0

Table D-5

REGIONWISE CONSTANTS AT 514°F

Region	C_B (ppm)	Thermal			Fast			
		Σ_a	$\nu\Sigma_f$	D	D	Σ_a	Σ_r	$\nu\Sigma_f$
Fuel	0	.11660	.17705	.36054	1.26653	.012872	.014126	.009485
	540	.12074	.17586	.36047	1.26676	.012975	.014041	.009477
	1080	.12485	.17471	.36037	1.26696	.013071	.013962	.009469
Water Slot	0	.0091052	---	.30664	1.52906	.00043827	.034761	---
	540	.018285	---	.30612	1.52929	.00064703	.034716	---
	1080	.027354	---	.30558	1.52949	.00085533	.034675	---
Zirconium	0	.0040563	---	.96353	1.28031	.00010476	.00021361	---
	540	.0040304	---	.96361	1.28037	.00010463	.00021333	---
	1080	.0040059	---	.96367	1.28042	.00010450	.00021308	---

APPENDIX E

CONTRIBUTION OF CONTROL RODS TO THE ABSORPTION CROSS SECTION OF THE CORE AT 514°F USING THE "SUPERCELL" REPRESENTATION OF CONTROL RODS

Table E-1

CONTRIBUTION OF CONTROL RODS TO THE ABSORPTION CROSS SECTION OF THE CORE AT 514°F USING THE "SUPERCELL" REPRESENTATION OF CONTROL RODS

	Fuel Assemblies/Control Rods			
Radial Region -- Rod Array	I	II	III	IV
0	0	0	0	0
1	4	0	0	0
51	4	0	6	0
351	4	4	6	0
2351	2	4	6	0
42351	2	2	6	0
642351	2	2	3	7

Fuel Assemblies/Control Rod	$(\Sigma_{aCR})_{Fast}$	$(\Sigma_{aCR})_{Thermal}$
2	.003917	.01628
3	.002519	.01000
4	.001857	.007223
6	.001217	.004638
7	.001038	.003934